TÜRKİYE CUMHURİYETİ
ADANA ALPARSLAN TÜRKEŞ SCIENCE AND TECHNOLOGY UNIVERSITY

GRADUATE SCHOOL
ELECTRICAL AND ELECTRONIC ENGINEERING DEPARTMENT

DESIGN AND SIMULATION OF QUASI-Z SOURCE INTEGRATED MULTILEVEL INVERTER FOR GRID CONNECTED SYSTEMS

ÇAĞATAY DENİZ IRMAK

M.Sc.

ADANA 2024

TÜRKİYE CUMHURİYETİ
ADANA ALPARSLAN TÜRKEŞ SCIENCE AND TECHNOLOGY UNIVERSITY

GRADUATE SCHOOL
ELECTRICAL AND ELECTRONIC ENGINEERING DEPARTMENT

DESIGN AND SIMULATION OF QUASI-Z SOURCE INTEGRATED MULTILEVEL INVERTER FOR GRID CONNECTED SYSTEMS

ÇAĞATAY DENİZ IRMAK

M.Sc.

THESIS ADVISOR
ASSOC. PROF. DR. TAHSİN KÖROĞLU

ADANA, 2024

DECLARATION OF CONFORMITY

In this thesis study, which was prepared following the thesis writing rules of Adana Alparslan Türkeş Science and Technology University Institute of Graduate School, I declare that I provide all the information, documents, evaluations and results in accordance with scientific ethics and moral codes without resorting to any means or assistance that would be contrary to scientific ethics and traditions. I also declare that I refer to all of the articles I used in this study with appropriate references and accept all moral and legal consequences if a situation is found contrary to my statement regarding my work.

02/08/2024

[Signature]

Çağatay Deniz IRMAK

ÖZET

ŞEBEKEYE BAĞLI SİSTEMLER İÇİN QUASI-Z KAYNAK ENTEGRELİ ÇOK SEVİYELİ EVİRİCİ TASARIMI VE SİMÜLASYONU

Çağatay Deniz IRMAK

Yüksek Lisans, Elektrik-Elektronik Mühendisliği Anabilim Dalı

Danışman: Doç. Dr. Tahsin KÖROĞLU

Ağustos 2024, 82 sayfa

Bu tez, şebekeye bağlı tek fazlı bir sistemde quasi-z-kaynak entegreli beş seviyeli evirici‘nin (QZKE) uygulamasına odaklanmakta ve önerilen yapının DC kaynak olarak bir yakıt hücresi ile arayüzlendiğinde çalışması incelemektedir. Minimum anahtar sayısına sahip QZKE, DC kaynak, şebeke ve çeşitli yükler arasında güç akışını yetkin bir şekilde yöneterek şebekeye bağlı uygulamalar için dikkat çekici bir çözüm sunmaktadır.

Modelleme yaklaşımı, QZKE sisteminin dinamik davranışını analiz etmek için MATLAB/Simulink kullanılarak yapılan detaylı simülasyon çalışmalarını içermektedir. Bu tez, QZKE ile yük değişimleri arasındaki etkileşimi çeşitli çalışma koşullarında ayrıntılı ve derinlemesine incelemektedir. Simülasyonlar, yakıt hücresi gücünün altında veya üzerindeki yük koşullarını içeren ve sistemin yalnızca şebeke ya da evirici modunda çalıştığı farklı çalışma modlarını kapsamaktadır. QZKE'nin verimlilik ve gerilim düzenleme açısından performansı, değişken yük durumları ele alınarak değerlendirilmiştir.

Bu detaylı inceleme ile QZKE teknolojisinin gerçek dünyadaki güç yönetimi performansını yüksek doğrulukla değerlendirmesi sağlanmaktadır. Bu tez, yenilenebilir enerji kaynaklarının entegrasyonu ve şebeke desteği potansiyelini göstererek QZKE teknolojisinin genel bakışına önemli bir katkı sunmaktadır. Önerilen sistem konfigürasyonunun uygulanabilir ve etkili olduğu, QZSI'nin değişken yük koşulları altında yüksek verimlilik ve düşük THD sağladığı simülasyon sonuçlarıyla ortaya konulmuştur.

Anahtar Kelimeler: Quasi-Z kaynak eviricisi (QZKE), Çok seviyeli evirici, Yakıt hücresi entegrasyonu, Şebekeye bağlı evirici

ABSTRACT

DESIGN AND SIMULATION OF QUASI-Z SOURCE INTEGRATED MULTILEVEL INVERTER FOR GRID CONNECTED SYSTEMS

Çağatay Deniz IRMAK

M.Sc., Department of Electrical and Electronic Engineering
Supervisor: Assoc. Prof. Dr. Tahsin KÖROĞLU

August 2024, 82 pages

This thesis focuses on implementing a quasi-z-source integrated five-level inverter (QZSI) in a grid-connected single-phase system, specifically examining its operation when interfaced with a fuel cell as the DC source. QZSI, with its minimal switch count, presents an attractive solution for grid-tied applications by proficiently managing the power flow between the DC source, grid, and various loads.

The modeling approach includes detailed simulation studies using MATLAB/Simulink to analyze the dynamic behavior of the QZSI system. This thesis thoroughly investigates the interaction between the QZSI and load variations under different operating conditions. Simulations cover scenarios where the fuel cell power is either below or above the load conditions, and when the system operates solely in the grid mode or in the inverter mode. The performance of the QZSI in terms of efficiency and voltage regulation was evaluated by considering variable load conditions.

This detailed examination allows for an accurate assessment of the real-world power management performance of QZSI technology. This thesis contributes significantly to the overall understanding of QZSI technology by demonstrating its potential for integrating renewable energy sources and providing grid support. Simulation results show that the proposed system configuration is feasible and effective, with the QZSI delivering a high efficiency and low THD under varying load conditions.

Keywords: Quasi-Z-source inverter (QZSI), Multilevel inverter, Fuel cell integration, Grid-connected inverter

Dedication

To my precious family and my girlfriend,

whose love, support, and encouragement have been my guidance.

ACKNOWLEDGEMENTS

I would like to express my deepest appreciation to my academic supervisor Assoc. Prof. Dr. Tahsin KÖROĞLU for his guidance and insight throughout this research.

I am also grateful to Research Assistant Elanur EKİCİ for her support and cooperation during my study.

I would also like to thank Assoc. Prof. Dr. N. Sinan ÖZBEK and Assoc. Prof. Dr. Doğan ÇELİK for accepting to be members of the examining committee for my thesis.

Finally, I would like to express my heartfelt gratitude to my parents, my brother and my girlfriend for their encouragement, patience and constant support.

TABLE OF CONTENTS

LIST OF FIGURES

LIST OF TABLES

LIST OF ABBREVIATIONS

AC	: Alternating Current
AFC	: Alkaline Fuel Cells
CBC	: Constant Boost Control
CSI	: Current Source Inverter
DC	: Direct Current
FP	: Fuel Pressure
FC	: Fuel Cell
LCL	: Inductor-Capacitor-Inductor Filter
MCFC	: Molten Carbonate Fuel Cells
MBC	: Maximum Boost Control
NPC	: Neutral Point Clamped
PAFC	: Phosphoric Acid Fuel Cells
PEMFC	: Proton Exchange Membrane Fuel Cells
PI	: Proportional and Integral
PLL	: Phase-Locked Loop
PV	: Photovoltaic
PDPWM	: Phase Disposition Pulse Width Modulation
QZSI	: Quasi-Z Source Inverter
QZS-MLI	: Quasi-Z Source Multilevel Inverter
SOFC	: Solid Oxide Fuel Cells
SPWM	: Sinusoidal Pulse Width Modulation
SBC	: Simple Boost Control
ST	: System Temperature
THD	: Total Harmonic Distortion
VSI	: Voltage Source Inverter

LIST OF SYMBOLS

V	**:** Voltage
I	**:** Current
P	**:** Power
Z	: Impedance
L	: Inductance
C	: Capacitance
R	: Resistance
F	: Frequency
ω	**:** Angular Frequency
θ	: Phase Angle
α	: Modulation Index
D	: Duty Cycle
Δ	: Difference or Change

1. INTRODUCTION

The increasing global demand for renewable energy sources demands a solution, which is expected to be the development of power conversion technologies mainly through its integration with existing electrical grids. The attention paid to Quasi-Z source inverters is tremendous in this regard, as they are part of these emerging technologies. Its ability to handle levels of input voltage is significantly wide thus offering flexible control of the flow of power. Unlike conventional inverters, QZSIs employ impedance networks with fewer passive components, thereby efficiently reducing cost, size and complexity.

Given this circumstance, the need to investigate the application of QZSIs in grid-connected single-phase systems with fuel cells as a DC power source motivated this research. Because fuel cells offer both a sustainable and transparent replacement for conventional power sources, they could serve as a viable option in stationary and portable power-generation applications. However, the integration of fuel cells into grid-connected systems could, be problematic because of their power-conversion control and grid synchronization.

The promising characteristics of QZSIs, paired with their operation capability in both buck and boost modes, overcome the challenges of conventional inverters. Thus, it realizes the transparent integration of fuel cells into the grid. Owing to its inherent capabilities, efficient management of the power flow between the grid, fuel cell, and loads can be achieved, ultimately providing reliability, stability, and grid compliance.

However, new issues have been introduced by new integrated sources of renewable energy, such as fuel cells. These include complications in the power conversion, grid synchronization and control. The expected result is the inability of some traditional inverters to offer the flexibility and efficiency needed for proper seamless integration, particularly in single-phase applications. This circumstance, necessitates further research on advanced power conversion technologies to address the challenges faced in the realization of the most effective way to utilize renewable energy sources.

The lack of literature regarding the applications of Quasi-Z source multi-level inverters (QZSIs) specifically in grid-connected single-phase systems, especially with fuel cells as the DC source of power, forms the motivation and subject of this thesis. Currently, the available literature only addresses three-phase QZSI systems, thus leaving a gap in our understanding of the feasibility and performance of QZSIs in single-phase configurations [1].

Therefore, this study will assist in filling the gap in the current literature and research on the performance of these systems within grid-connected environments, with a particular focus on single-phase operation and fuel cell integration. Thus, this research aims to conduct an in-depth simulation study of the QZSI under different operating conditions and load scenarios using Simulink to display and validate the dynamic behavior. The results and conclusions could further help develop QZSI technology and provide it for real applications in actual renewable energy systems. The main objectives of this research are as follows:

Model Development: A detailed simulation model of a single-phase QZSI system integrated with a fuel cell and grid connection will be developed using Simulink.

Performance Analysis: Evaluate the dynamic behavior and performance of the QZSI system under varied operating conditions, including different loading conditions and grid disturbances.

Stability Assessment: Analyze the stability and grid synchronization capability of the QZSI system, particularly when it is subjected to a change in load demand and grid conditions.

Efficiency Assessment: Carry out the efficiency and energy conversion performance evaluation of the QZSI system, concerning power losses and voltage regulation, given the effects of harmonic distortion.

Grid Interaction: The interaction of QZSI systems, a fuel cell, and the grid is outlined relative to power flow control, voltage regulation, and grid support functions.

The latter will fulfill the beforementioned objectives for the QZSI technology furtherance as well as gain valuable insight into its potential application within grid-connected single-phase systems using renewable sources of energy. The data and findings gained from this study should enable further development of power conversion solutions for a reliable and efficient integration into energy sustainability.

1.1. Inverters

Inverters play a crucial role in power conversion systems, as they convert direct current (DC) into alternating current (AC) through a process known as switching. The conversion of power is used for various applications, from household appliances to industrial drives, as well as in renewable energy systems. Therefore, several types of inverters are designed that satisfy the specific requirements which use different modulation techniques to ensure controlled and efficient power conversion.

1.1.1. Working Principles of Inverters

The basic function of an inverter is to produce an AC output from a DC input. This is done by rapidly switching semiconductor devices on and off, for example IGBTs (Insulated Gate Bipolar Transistors) or MOSFETs (Metal-Oxide-Semiconductor Field-Effect Transistors), a control circuit, as well as passive components like inductors and capacitors. During this rapid but precise switching sequence, voltage pulses are produced. After proper filtering, for which passive components tailored to the inverter's needs are employed to remove high-frequency components, the voltage pulses are shaped into smooth sinusoidal waveforms suitable for AC loads. As mentioned before, an inverter's implementation and design can vary significantly based on its intended function and application. The main differences, however, lie in their input and output characteristics, modulation methods and control strategies [2].

The control circuit in an inverter is responsible for the generation of appropriate switching signals based on the desired frequency and output voltage. To enhance the performance of the inverter, advanced control algorithms are often implemented. These can, for example, maintain a constant output under varying load conditions and additionally minimize power losses. These control strategies are a crucial factor for an efficient and stable inverter operation, particularly in applications in which precise power control is necessary.

In order to monitor current and output voltage, feedback mechanisms are commonly integrated into inverter systems. These mechanisms are used to dynamically adjust the switching patterns, thus ensuring a stable output that remains within the desired parameters. Proportional-Integral (PI) controllers are often utilized in the feedback loop to regulate the output [3]. As they provide continuous adjustment to the inverter's operation, optimal performance can be maintained.

In summary, the working principle of inverters involves a rapid, but controlled, switching of semiconductor devices to convert direct current (DC) into alternating current (AC). With the use of additional filtering and feedback mechanisms, a stable and high-quality output is ensured. These techniques are essential for the efficient operation of inverters in various applications in need of precise and reliable power conversion, ranging from industrial motor drives to renewable energy systems.

1.1.2. Types of Inverters

Inverters can generally be divided into different types based on their configurations and applications, as well as how each type stores and manages energy. Additionally, they can be differentiated based on their specific applications and operational characteristics.

A common type of inverter is the Voltage Source Inverter, VSI for short. It stores energy via capacitors, thus providing a constant voltage output. For this reason, VSIs are frequently used in applications requiring a stable voltage, such as uninterruptible power supplies (UPS) and grid-tied renewable energy systems. Although simple yet effective, according to [4], they potentially lack the effectiveness and ability to boost the voltage.

Another common type is the Current Source Inverter (CSI). This inverter type stores energy through inductors, providing a constant output current. This makes it suitable for sensitive operations and applications that require precise current control, such as motor drives and industrial processes. The large inductors required for CSIs make them typically more complex and bulkier than VSIs [5].

Multilevel inverters represent another important category of inverters. These inverters, by using multiple voltage levels, can produce a high-quality AC output with reduces harmonic distortion and can thus achieve better performance and efficiency. This characteristic makes them particularly beneficial for high-power applications such as high-power industrial drives, as well as large scale renewable energy installations [6]. These inverters, however, require more complex control and a higher amount of components [7].

1.1.3. Modulation Methods

The modulation techniques used by inverters are crucial for their efficiency and performance. These methods are responsible for regulating the switching of semiconductor devices to achieve the desired frequency and output voltage, while at the same time minimizing harmonic distortion.

A common technique is Pulse Width Modulation (PWM). This technique's ability to vary the width of the voltage pulses allows it to efficiently control the output voltage and frequency. PWM compares a reference signal with a high-frequency triangular carrier signal, with the points at which the two signals intersect determining the switching instant of the semiconductor devices.

Another commonly used technique, The Sinusoidal Pulse Width Modulation (SPWM) simply, yet effectively, controls the output voltage and minimizes harmonic distortion. It achieves so by following a similar pattern as PWM, but this time comparing a sinusoidal reference signal representing the desired AC output to the triangular carrier signal which sets the switching frequency [8]. This method allows for precise control over the output of the inverter and is particularly effective at reducing the total harmonic distortion (THD) in the output waveform. This results in cleaner and more stable AC supply.

The Space Vector Pulse Width Modulation (SVPWM), one of more advanced techniques, offers improved performance as it optimizes the switching sequence of the inverter, resulting in lower switching losses, higher output voltage, minimizing harmonic distortion and improving efficiency. This modulation involves representing the three-phase voltage as vectors in a two-dimensional plane and determining the switching states which would best approximate the desired output vector. SVPWM's ability of achieving better utilization of the DC bus voltage results in higher output voltage compared to SPWM. This is particularly advantageous in three-phase inverters, providing a smoother and more efficient operation.

The Hysteresis Band Current Control (HBCC) is a modulation method that maintains the output current within a pre-defined hysteresis band around the reference current. The inverter's switches are controlled in order to keep the current within this band, providing a good current regulation and a fast dynamic response. The switching frequency can vary, however, leading to increased electromagnetic interference (EMI) and potentially to challenged in filter design. Nevertheless, HBSS is often used despite these challenges in application that require precise current control, such as active power filter and motor drives.

Another modulation method is the Pulse Amplitude Modulation (PAM). It involves varying the amplitude of the pulses according to the amplitude of the reference signal. PAM adjusts the height of the pulses, unlike PWM, which adjusts the pulse width. This may make it simpler, but less effective in reducing harmonic distortion compared to other PWM techniques. Due to its higher THD and lower efficiency, it is not used as commonly in modern inverter designs but can still be found in specific low-cost applications in which simplicity is prioritized.

Delta Modulation (DM) uses the error between the reference signal and the output signal to generate switching pulses. This results in a modulated output that closely follows the reference signal. This method offers simplicity in implementation, yet high dynamic performance. It can, however, suffer from high switching losses and noise. It is particularly suitable for applications that require a rapid response to changes in reference signal, such as certain types of power converters or dynamic voltage restorers.

In order to ensure effective control of inverters, modulation methods are essential. Techniques like SPWM, SVPWM, HBCC, PAM and DM have their own unique applications and (dis)advantages. SPWM remains the most widely used due to its simplicity and effectiveness in the reduction of harmonic distortion. More advances methods such as SVPWM, however, offer a more improved performance in specific applications.

Additionally to these types and methods, inverters can be designed for special functions. An example would be grid-tied inverters, which synchronize with the grid to supply excess power from renewable sources, as well as standalone inverters which operate independently from the grid to supply power to isolated loads. Several factors, such as the desired efficiency, the specific requirements and the type of load, influence which modulation technique and inverter type are chosen for the application.

1.2. Quasi-Z Source

QZSIs are an advanced type of inverter that includes an impedance network consisting of inductors and capacitors. This enables both buck and boost operation, allowing the converter to handle a wide range of input voltages without additional components such as transformers.

QZSI is a relatively recent advancement in power electronics that offers unique properties and advantages over traditional voltage source inverters (VSI) and current source inverters (CSI). The QZSI topology, first introduced by Fang Zheng Peng in [9], uses a unique impedance network that enables bidirectional power flow and voltage boost while requiring fewer components.

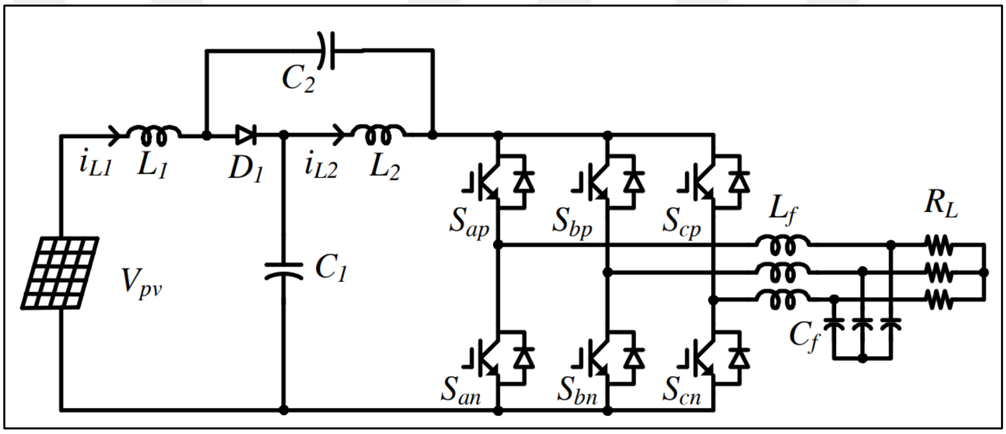

Figure 1.1. QZSI in the PV power generation system in [9].

The impedance network is at the heart of a QZSI and in most cases comprises two inductors and capacitors interconnected to form a specific configuration. This network allows the inverter to perform voltage boosting without requiring a bulky and expensive transformer based solution. QZSI employs this impedance network that can cope well with the varying voltage level at input, which renders it a compatible option for diverse renewable energy applications including photovoltaic (PV) systems, wind turbine and fuel cells.

One of the most prominent features available with QZSI is to work in both buck and boost modes enabling seamless power conversion between different voltage levels. This feature is particularly useful for grid-connected systems where the input voltage can change on account of fluctuations in renewable energy sources or grid disturbances. The QZSI also features inherent shoot-through protection to minimize short-circuit fault risks, thus ensuring system reliability.

The significance of QZSIs in renewable energy systems lies in their ability to overcome many of the limitations associated with traditional inverters. By providing bidirectional power flow and voltage boost capabilities, QZSIs enable efficient utilization of renewable energy sources, grid support functions, and integration with energy storage systems. Furthermore, the simplified topology of QZSIs results in reduced cost, size, and complexity, making them an attractive solution for both residential and commercial applications.

Overall, the QZSI represents a significant advancement in power electronics technology with promising implications for the integration of renewable energy sources into the electrical grid. Understanding the principles and characteristics of QZSIs is essential for harnessing their full potential and advancing the development of sustainable energy systems.

1.2.1. Working Principle of QZSIs

Their unique impedance network causes QZSIs to deliver higher voltage gains and better efficiency than conventional inverters. Mathematical modeling is the first and most important issue of designing a QZSI. The state-space equations will be developed to represent dynamical behavior of the system. These equations consider the unique impedance network in QZSI with a combination of inductors and capacitors, enabling both buck & boost operations within single stage power conversion.

The state-space averaging method is commonly used to derive the small-signal model of QZSIs. This method involves linearizing the nonlinear system equations around an operating point to obtain a set of linear differential equations that approximate the system's behavior. The state-space representation of the QZSI can be expressed as:

$$x^{\cdot}(t) = A \cdot x(t) + B \cdot u(t) \tag{1}$$

$$y(t) = C \cdot x(t) + D \cdot u(t) \tag{2}$$

where:

- x(t) represents the state variables, including inductor currents and capacitor voltages.
- u(t) is the input vector, including the input voltage and the control inputs such as the shoot-through duty cycle.
- y(t) is the output vector, representing the output voltage and current.
- A, B, C, and D are matrices that describe the system dynamics [10].

The operation of QZSIs is governed by nonlinear differential equations due to the presence of the impedance network and the switching actions. These equations can be derived for both the shoot-through and non-shoot-through states.

During the shoot-through state, the switches are simultaneously turned on, creating a short circuit through the DC link. The energy stored in the inductors is transferred to the capacitors, boosting the output voltage. The equations for the shoot-through state are:

$$L\frac{di_L}{dt} = V_{in} - V_L \quad (3)$$

$$C\frac{dV_C}{dt} = i_L - i_C \quad (4)$$

During the non-shoot-through state, the inverters operate normally, and the energy is transferred from the capacitors to the load. The equations for the non-shoot-through state are:

$$L\frac{di_L}{dt} = V_{in} - V_C \quad (5)$$

$$C\frac{dV_C}{dt} = i_L - i_{load} \quad (6)$$

The transfer function of the QZSI can be obtained by taking the Laplace transform of the state-space equations. This provides a frequency-domain representation of the system, which is useful for control design and stability analysis [11]. The transfer function H(s) of the QZSI can be expressed as:

$$H(s) = \frac{N(s)}{D(s)} \tag{7}$$

Where N(s) and D(s) are the numerator and denominator polynomials, respectively, derived from the state-space equations [12].

1.2.2. Shoot-Through Control

Shoot-through control in QZSIs is a pivotal strategy that enhances the reliability and protects the system from short-circuit faults. This method involves the intentional short-circuiting of the inverter legs, which might seem counterintuitive at first glance. However, this controlled short-circuiting allows the inductor current to flow freely and charge the capacitors, effectively boosting the output voltage. The energy stored in the inductors during the shoot-through period is transferred to the capacitors, which subsequently increases the voltage available at the inverter's output. This mechanism enables the QZSI to handle a wide range of input voltages and provides a higher degree of control over the output voltage, making it an efficient and robust solution for power conversion.

The modulation index control in QZSIs is also crucial for maintaining the desired output voltage and improving the overall efficiency of the system. The modulation index determines the amplitude of the output voltage relative to the DC input voltage. By adjusting the modulation index, the inverter can adapt to variations in the input voltage and load conditions, ensuring consistent performance. This adaptability is particularly important in applications involving renewable energy sources, where input voltages can fluctuate significantly. The ability to dynamically adjust the modulation index allows the QZSI to maintain optimal operation, minimize power losses, and enhance overall system efficiency.

Furthermore, shoot-through control contributes to the inverter's ability to operate in both buck and boost modes. In buck mode, the inverter steps down the voltage, while in boost mode, it steps up the voltage. The seamless transition between these modes is facilitated by the shoot-through state, which provides the necessary voltage boost without the need for additional components like transformers. This capability is essential for applications that require a wide range of operating voltages, such as photovoltaic systems, fuel cells, and other renewable energy applications.

In addition to voltage boosting, shoot-through control also improves the inverter's fault tolerance. Traditional inverters are vulnerable to short-circuit faults that can damage the system and lead to operational failures. In contrast, the QZSI's inherent shoot-through capability allows it to safely handle short-circuits by directing the fault current through the shoot-through path, thereby protecting the inverter's components from damage. This fault-tolerant design enhances the overall reliability and longevity of the inverter, making it suitable for use in critical applications where system stability and durability are paramount.

Overall, shoot-through control is a fundamental aspect of QZSI operation, providing significant benefits in terms of voltage boosting, fault tolerance, and adaptability to varying input conditions. By integrating shoot-through control with precise modulation index adjustments, QZSIs achieve superior performance and efficiency, making them an ideal choice for modern power conversion applications.

1.3. Fuel Cells

Fuel cells are electrochemical converts that transform chemical energy into electrical energy through the reaction of fuel and oxidant. They offer a clean and efficient alternative to traditional power generation methods. The potential applications span from portable electronics and vehicles to stationary power generation systems.

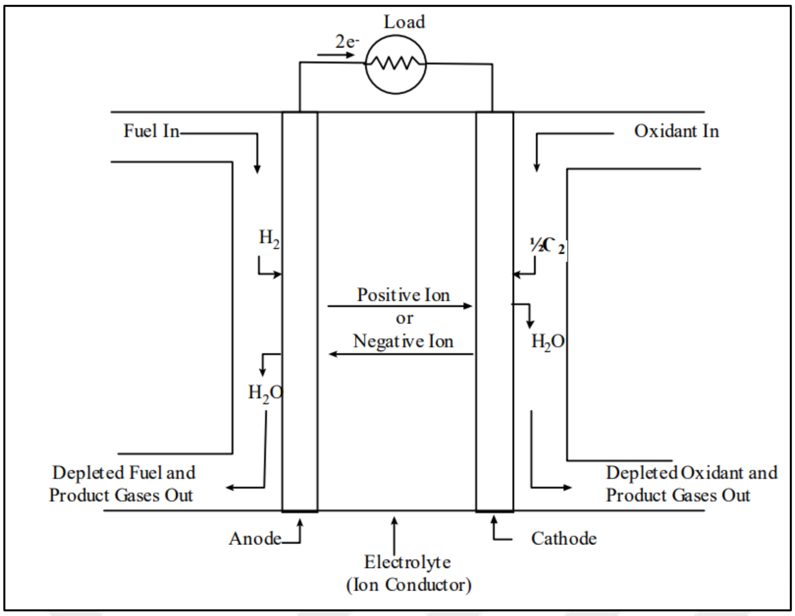

Figure 1.2. Schematic of an individual fuel cell [13].

The most common fuel cells include proton exchange membrane fuel cells (PEMFCs), alkaline fuel cells (AFCs), phosphoric acid fuel cells (PAFCs), solid oxide fuel cells (SOFCs), and molten carbonate fuel cells (MCFCs). The mentioned types of fuel cells have unique characteristics in terms of operating temperature, electrolyte material, and fuel compatibility, allowing for diverse applications across different industries [13],[14],[15],[16],[17]. Fuel cells can operate on different fuels, including hydrogen, methanol, natural gas, and biogas.

Hydrogen fuel cells, in particular, have garnered significant focus due to their high energy density, zero emissions, and potential for renewable hydrogen production through electrolysis using renewable energy sources. In grid-connected systems, fuel cells serve as a reliable and sustainable DC power source for feeding into inverters for AC power conversion. The DC output of the fuel cell is typically conditioned and regulated to match the requirements of the connected loads or grid interface. This role as a DC source is crucial for integrating fuel cells into renewable energy systems and enabling seamless power conversion and distribution.

The advantages of fuel cells as a DC power source include high efficiency, low emissions, modularity, and scalability. They offer stable and continuous power output, making them suitable for both grid-connected and standalone applications, including backup power systems, distributed generation, and microgrids. Furthermore, fuel cells can operate independently of ambient conditions, providing reliable power generation in remote or harsh environments.

Despite their numerous advantages, fuel cells also face challenges such as high capital costs, limited infrastructure, and issues related to hydrogen storage and distribution. Research and development efforts are ongoing to address these challenges and enhance the performance, reliability, and cost-effectiveness of fuel cell technology.

1.3.1. Types of Fuel Cells

Fuel cells are classified into several types based on the electrolyte used and the operating temperature, each with unique characteristics:

- **Proton Exchange Membrane Fuel Cells (PEMFCs):** Operates at low temperatures and use a polymer electrolyte membrane. Known for high power density and quick start-up times [13].
- **Alkaline Fuel Cells (AFCs):** Uses an alkaline electrolyte like potassium hydroxide. They have high efficiency but are sensitive to CO2 contamination [14].
- **Phosphoric Acid Fuel Cells (PAFCs):** Operates at moderate temperatures and use phosphoric acid as the electrolyte. Primarily used in stationary power generation applications [15].
- **Solid Oxide Fuel Cells (SOFCs):** Operates at high temperatures and use a solid ceramic electrolyte. Suitable for high-efficiency power generation [16].
- **Molten Carbonate Fuel Cells (MCFCs):** Operates at high temperatures and use a molten carbonate electrolyte. Efficient and can utilize various fuels, including natural gas and biogas [17].

1.3.2. Working Principle of Fuel Cells

Fuel cells generate electricity through an electrochemical reaction between a fuel, typically hydrogen, and an oxidant, usually oxygen. This process involves the fuel cell's two primary components: the anode and the cathode, separated by an electrolyte. At the anode, hydrogen molecules are split into protons and electrons through a catalytic reaction. The protons pass through the electrolyte to the cathode, while the electrons travel through an external circuit, creating an electric current that can be used to power electrical devices.

At the cathode, the protons and electrons recombine with oxygen molecules in another catalytic reaction to form water, which is the primary byproduct of the process. Additionally, this reaction produces heat, which can be utilized in combined heat and power (CHP) systems to increase overall energy efficiency.

The efficiency of fuel cells is generally higher than traditional combustion-based power generation methods because they directly convert chemical energy into electrical energy without the intermediate step of generating heat, which is then converted into mechanical energy and subsequently into electricity. This direct conversion process minimizes energy losses, making fuel cells an attractive option for clean energy production.

Fuel cells also offer significant environmental benefits as they produce electricity with low or zero emissions, depending on the fuel source. When hydrogen is derived from renewable sources, the entire process can be nearly emission-free, contributing to the reduction of greenhouse gases and other pollutants.

Moreover, fuel cells are highly scalable, allowing for applications ranging from small portable devices to large power plants. They can be used in stationary applications, such as backup power systems and distributed generation, as well as in mobile applications, including fuel cell vehicles and portable power units. The versatility and environmental benefits of fuel cells make them a promising technology for meeting future energy demands sustainably.

1.4. Output Filter Types

To ensure the AC output of an inverter is suitable for grid connection, output filters are employed to remove high-frequency harmonics and produce a sinusoidal waveform. Different types of output filters are utilized, each with specific characteristics and advantages. The primary types of inverter output filters include LC filters, LCL filters, and higher-order filters such as LCLC and RLC filters.

LC filters are the simplest form of output filters, consisting of an inductor (L) and a capacitor (C). These filters provide basic low-pass filtering, attenuating high-frequency harmonics generated by the switching operations of the inverter. The design of LC filters involves selecting appropriate values for the inductance and capacitance to achieve the desired cutoff frequency and attenuation characteristics. However, LC filters may not be sufficient for applications requiring stringent harmonic suppression due to their limited filtering capabilities [18].

LCL filters are more advanced than LC filters and are widely used in grid-connected inverters. An LCL filter consists of two inductors (L1 and L2) and a capacitor (C) arranged in an LCL configuration. This filter type offers superior harmonic attenuation compared to LC filters, providing significant reduction in total harmonic distortion (THD). The LCL filter's design involves careful selection of the inductance and capacitance values to balance filtering performance and system stability. The inclusion of a damping resistor may be necessary to mitigate resonance issues and ensure stable operation [19].

The LCL filter stage is critical for reducing harmonics in the output of the inverter. An LCL filter consists of two inductors and a capacitor, which form a low-pass filter to attenuate high-frequency components. The design of the LCL filter must balance the trade-off between filtering performance and system stability.

The LCL filter, composed of two inductors and a capacitor, forms a low-pass filter that effectively reduces the total harmonic distortion (THD) in the output voltage and current. The design and optimization of the LCL filter are critical to ensuring the stability and efficiency of the grid-connected inverter system.

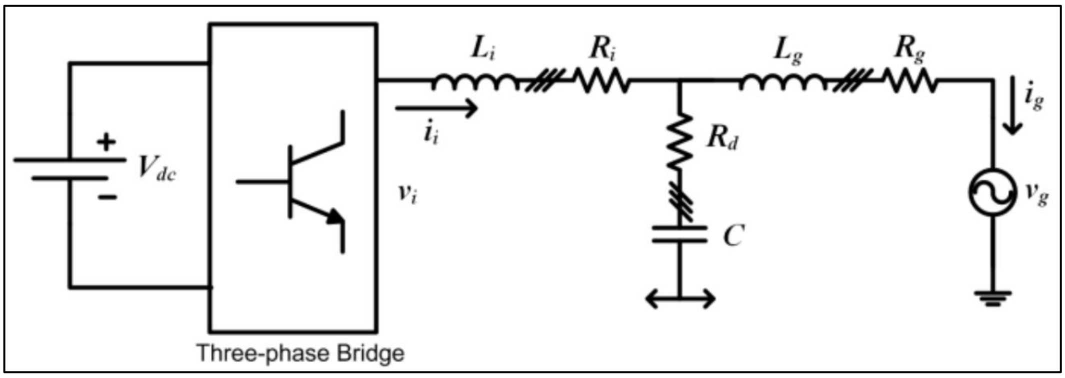

Figure 1.3. General structure of three-phase VSI with LCL-filter in [19].

LCLC filters incorporate an additional LC stage to further enhance harmonic attenuation. This configuration consists of two inductors and two capacitors arranged in a specific manner to form a fourth-order filter. The LCLC filter provides even greater attenuation of high-frequency harmonics, making it suitable for applications requiring very low THD. The design complexity of LCLC filters is higher, and careful consideration must be given to the component values and the potential for resonance issues [20].

RLC filters combine resistors (R), inductors (L), and capacitors (C) to provide comprehensive filtering capabilities. These filters are particularly effective in reducing both high-frequency harmonics and resonant peaks. The inclusion of resistors helps to dampen resonance and improve the stability of the filter. RLC filters are commonly used in applications where both differential mode and common mode noise need to be mitigated. The design of RLC filters involves balancing the trade-offs between filtering performance, power loss, and component cost [21].

Advanced filter designs include variations such as self-tuning filters and envelope-type (E-type) modules. Self-tuning filters automatically adjust their parameters to track and attenuate harmonic components effectively, which is beneficial in systems with variable output frequencies. E-type modules reduce the number of components while maintaining high-quality output, making them efficient for modular inverter designs [22],[23].

1.5. Grid Connection

Grid-connected systems involve synchronizing the inverter output with the grid, a process that demands precise control over the inverter's voltage, frequency, and phase to ensure alignment with the grid parameters. This synchronization is very important for maintaining the stability and efficiency of the power supply. In grid-connected mode, the inverter can export excess power generated by renewable sources, such as solar panels or fuel cells, to the grid, thereby contributing to the overall energy supply and reducing dependence on fossil fuels. Conversely, during periods when the renewable energy sources are insufficient to meet the load demand, the inverter can draw power from the grid to ensure a continuous and reliable power supply to the connected loads. This bidirectional power flow enhances the flexibility and reliability of the energy system, allowing for efficient energy management and optimal utilization of renewable resources.

1.5.1. Types of Grid Connections for Inverters

Direct grid connection involves connecting the inverter directly to the utility grid. This method requires the inverter to continuously monitor and adjust its output to match the grid's voltage, frequency, and phase. The direct connection ensures that any excess power generated by renewable sources can be immediately fed into the grid. It also allows the system to draw power from the grid when the renewable sources are insufficient. The primary challenge of direct grid connection is maintaining synchronization and ensuring that the inverter's output does not disrupt the grid's stability.

Indirect grid connection typically involves the use of transformers or other intermediary devices to connect the inverter to the grid. This method can provide isolation between the inverter and the grid, which enhances safety and reduces the risk of electrical faults. Transformers can also help match the voltage levels of the inverter output and the grid, ensuring efficient power transfer. Indirect grid connection is particularly useful in applications where there are significant differences in voltage levels or where additional protection is required.

Microgrid integration involves connecting the inverter to a localized grid that can operate independently or in conjunction with the main utility grid. In a microgrid setup, the inverter not only synchronizes with the main grid but also manages the power flow within the microgrid. This setup allows for greater control over local energy resources and enhances the resilience of the power supply. During normal operation, the microgrid can exchange power with the main grid. However, in case of grid outages, the microgrid can operate in an islanded mode, ensuring uninterrupted power supply to critical loads.

Hybrid systems combine grid-connected inverters with other energy storage or generation technologies, such as batteries or diesel generators. In these systems, the inverter not only manages the synchronization with the grid but also optimizes the use of different energy sources to ensure a reliable and efficient power supply. For instance, during peak solar generation periods, excess power can be stored in batteries and later used when solar generation is low.

Hybrid systems offer a versatile solution for enhancing grid stability and maximizing the use of renewable energy.

Virtual synchronous generators are advanced inverters that mimic the behavior of traditional synchronous generators. VSGs can provide inertia to the grid, enhancing its stability and robustness. By emulating the mechanical properties of conventional generators, VSGs can help smooth out fluctuations in power supply and support grid frequency regulation. This method is particularly useful in high-penetration renewable energy systems where maintaining grid stability is challenging.

1.5.2. Current Control and Synchronization Methods

Current control methods are critical for the efficient and stable operation of grid-connected inverter systems. These methods ensure that the inverter can accurately regulate the output current, maintain synchronization with the grid, and respond effectively to varying load conditions. The main objectives of current control in inverter systems include maintaining the desired output current waveform, minimizing harmonic distortion, and ensuring robust operation under different grid and load scenarios.

There are several types of current control methods, each with distinct control strategies and implementation techniques. One of the simplest and most widely used methods is PI control. PI control involves two components: proportional control, which produces an output proportional to the current error (the difference between the desired and actual current), and integral control, which produces an output proportional to the integral of the current error. The proportional component helps reduce the error quickly, while the integral component eliminates steady-state errors, improving accuracy over time. In grid-connected systems, PI controllers are often used in conjunction with DQ transformation to regulate the D and Q components of the current separately, ensuring precise control of active and reactive power.

The DQ transformation, also known as the Park transformation, is another method for current control. It simplifies the control of AC currents by converting them from the stationary reference frame (abc) to a rotating reference frame (dq0), transforming sinusoidal waveforms into DC quantities. The DQ transformation can be expressed as the following:

$$\begin{bmatrix} I_d \\ I_q \end{bmatrix} = \begin{bmatrix} cos(\theta) & in(\theta) \\ sin(\theta) & cos(\theta) \end{bmatrix} \begin{bmatrix} I_a \\ I_b \end{bmatrix} \tag{8}$$

This transformation involves converting the three-phase currents (Ia, Ib, and Ic) into two orthogonal components, I_d (direct axis) and I_q (quadrature axis), using a transformation matrix. The I_d component corresponds to the active power, while the I_q component corresponds to the reactive power. By independently controlling I_d and I_q, the inverter can effectively manage the active and reactive power output. The DQ transformation simplifies the control algorithm, enhances the accuracy and responsiveness of current control, and facilitates decoupled control of active and reactive power, improving overall system performance and stability.

A Phase-Locked Loop (PLL) is essential for synchronizing the inverter output with the grid. The PLL ensures that the inverter's output phase matches the grid phase, which is crucial for stable and efficient grid-connected operation. The PLL detects the phase angle of the grid voltage and generates a reference signal that aligns the inverter's output phase with the grid. It consists of a phase detector, a loop filter, and a voltage-controlled oscillator (VCO). The phase detector compares the grid voltage phase with the inverter's output phase and generates an error signal. The loop filter processes the error signal and adjusts the VCO to minimize the phase difference, achieving synchronization. PLL ensures accurate phase synchronization between the inverter and the grid, improves the quality of power transfer by minimizing phase errors, and enhances the inverter's ability to respond to grid disturbances and maintain synchronization under varying conditions. The equation of the used PLL for phase detection:

$$\theta(t) = \int_0^t \omega_{grid}(\tau) d \tag{9}$$

Hysteresis current control is a feedback control method that maintains the output current within a predefined hysteresis band around the reference current. The inverter switches are controlled to keep the current within the hysteresis band, resulting in a near-instantaneous response to current deviations. This method provides fast dynamic response and precise current regulation, and it is simple to implement and highly effective for applications requiring tight current control. However, the switching frequency can vary, leading to increased electromagnetic interference (EMI) and challenges in filter design.

1.6. Background and Research Motivation

The increasing utilization of renewable energy sources raises the urgent need for advanced power conversion technologies. A QZSI bears a number of practical advantages over the conventional inverters, involving reduced component count, cost and complexity, with flexible power flow control.

Fuel cells, which provide a clean and efficient DC power source, are promising alternatives for both stationary and portable power generation applications. Combining fuel cells with QZSIs in grid-tied systems would solve the challenges in control and synchronization encountered in the power conversion process.

1.7. Objectives of the Thesis

The general objective of this research is to investigate the application of Quasi-Z Source Inverters (QZSIs) to grid-connected single-phase systems with fuel cells. To achieve this, the research has several specific objectives. The first objective is model development, which involves creating a detailed simulation model of a single-phase QZSI system with integrated fuel cells and grid connection using Simulink. This model will serve as a foundation for analyzing the system's behavior and performance. The second objective is performance analysis, where the dynamic behavior and performance of the QZSI system will be investigated under various operating conditions, including changes in loading conditions and grid disturbances. This analysis will help us understand how the system responds to different scenarios.

The third objective is stability assessment, focusing on analyzing the stability and grid synchronization capability of the QZSI system. Special consideration will be given to changes in load demand and grid conditions to ensure that the system remains stable and synchronized with the grid. The fourth objective is efficiency evaluation, which involves analyzing the efficiency and energy conversion performance of the QZSI system. This includes assessing power losses and voltage regulation while accounting for the impact of harmonic distortion on overall system performance.

Lastly, the fifth objective is grid interaction, where the research will describe the interactions between the QZSI systems, fuel cells, and the grid. This includes examining power flow control, voltage regulation, and grid support functions to ensure seamless integration and optimal performance of the system. Collectively, these objectives aim to provide a comprehensive understanding of the application of QZSIs in grid-connected single-phase systems with fuel cells, highlighting their potential benefits and addressing potential challenges.

1.8. Outline of the Thesis

This thesis is organized into several chapters, each addressing specific aspects of the research topic. The Introduction chapter provides an overview of the research problem, motivation, and objectives, outlining the significance of the study and providing a roadmap for the subsequent chapters. The Literature Review chapter offers a comprehensive review of existing literature on Quasi-Z Source Inverters (QZSIs), single-phase inverters, grid connections, and fuel cells. It examines previous research studies, identifies gaps in the literature, and establishes the theoretical foundation for the research.

The Materials and Methods chapter details the simulation setup using Simulink, including the development of the QZSI model, the integration of the fuel cell as the DC source, and the configuration of load scenarios. This chapter explains the simulation procedures used to analyze the performance of the QZSI system. The Analysis and Discussion chapter presents the simulation results and parameters. This chapter analyzes the performance of the QZSI system, focusing on voltage regulation, power flow control, and grid interaction for various load scenarios and operating conditions. It discusses the implications of the findings and compares them with theoretical expectations.

The Conclusion chapter summarizes the main findings of the study, highlighting the contributions to the field of power electronics and renewable energy integration. This chapter also provides recommendations for further research and concludes the thesis.

2. LITERATURE REVIEW

QZSIs have garnered significant attention for their unique ability to integrate renewable energy sources, such as PV panels and fuel cells, into the grid. The QZSI topology is particularly beneficial for applications requiring single-phase inverters and minimal switching components. This study aims to comprehensively cover the advancements and research trends in QZSI, single-phase inverters, and their grid connections, especially focusing on systems using fuel cells as power sources.

2.1. Single-Phase Inverters

Single-phase inverters play a crucial role in connecting renewable energy sources, such as PV panels and fuel cells into the power system on residential level or small commercial applications. An overview is provided of QZSIs for these applications, emphasizing their advantages related to the reduced component ratings or continuous input current and improved power quality [24],[25].

Enhancements in single-phase inverter performance have been achieved through advanced control techniques and innovative designs. For instance, a hybrid PWM technique has been proposed to reduce power loss and improve system efficiency by dynamically adjusting the modulation strategy based on the operating conditions [26].

2.2. Multilevel Inverters

Multilevel inverters greatly improve power quality due to the voltage levels synthesized from multiple DC voltage levels, and thus decrease the total harmonic distortion (THD) and improve efficiency. Modern power systems require these kinds of inverters due to their potential for handling high voltages and currents. This makes them ideal to integrate renewable energy resources, such as PV systems and wind turbines, into the grid [27].

Advancements in multilevel inverter technology include various topologies like diode-clamped, flying capacitor, cascaded H-bridge, and Neutral Point Clamped (NPC) inverters. Diode-clamped inverters are noted for their simple structure and high-power application effectiveness, though they require numerous clamping diodes for higher voltage levels [28].

NPC inverters, utilizing clamping diodes to connect the neutral point to the middle of the DC bus, produce three voltage levels (positive, zero, and negative). This reduces the voltage stress on power switches, improves harmonic performance, and enhances system reliability [29].

Control strategies, such as space vector PWM (SVPWM), selective harmonic elimination (SHE), and multicarrier PWM techniques like phase disposition (PD), phase opposition disposition (POD), and alternate phase opposition disposition (APOD) are critical for minimizing switching losses and maintaining voltage balance. These techniques aim to optimize the inverter's performance under various operating conditions [30]. Recent studies have explored advanced control methods like model predictive control (MPC) and AI-based approaches to enhance dynamic response and reliability [31].

Applications of multilevel inverters extend to industrial drives, grid-tied systems, and electric vehicle (EV) charging stations, where their efficiency and power quality benefits are highly valued [32]. For instance, cascaded H-bridge inverters are commonly used in large-scale PV integration due to their modularity and scalability, offering effective power balance and high efficiency [33].

2.3. Quasi-Z Source Inverters

QZSIs have evolved from traditional Z-source inverters to address the limitations of conventional voltage-source and current-source inverters. The QZSI employs a unique impedance network, comprising inductors and capacitors, to achieve voltage buck-boost capability in a single-stage power conversion, enhancing the efficiency and reliability of power systems [34]].

Control strategies for QZSIs are pivotal in maximizing the efficiency and stability of grid-connected systems. Various studies have explored different control techniques such as sliding mode control (SMC), adaptive neuro-fuzzy inference systems (ANFIS), and hybrid pulsewidth modulation (HPWM) to regulate output power and ensure efficient operation under varying conditions [35],[36],[37].

2.4. Fuel Cell-Based Systems

Fuel cells, as a renewable energy source, are increasingly integrated into power systems using QZSIs due to their high efficiency and low environmental impact. The QZSI topology's ability to provide voltage buck-boost in a single stage makes it ideal for fuel cell applications, enhancing the overall system reliability and performance [38].

2.5. Grid Connections

Transformerless grid-tied inverters have become popular due to their reduced size, weight, and cost. The QZSI topology is particularly advantageous for transformerless applications because it minimizes common-mode leakage currents, a significant issue in grid-connected systems [39], [40].

Ensuring grid stability and maintaining power quality are critical challenges addressed by modern QZSIs. Techniques like space vector modulation (SVM) and active power decoupling have been proposed to improve the dynamic performance and reduce harmonic distortions in grid-tied systems [41], [42].

2.6. Summary of previous research on similar topics

QZSI have been developed to improve upon traditional Z-source inverters. These inverters are known for their single-stage power conversion capability, which allows both voltage buck and boost. The QZSI topology is especially useful in applications involving renewable energy sources, such as photovoltaic (PV) panels and fuel cells, due to its efficiency and reliability [43],[44],[45].

Effective control strategies are essential for optimizing the performance of QZSIs, particularly in grid-connected systems [46]. Single-phase inverters are integral for residential and small commercial applications, especially when integrating renewable energy sources:

- **Non-isolated Semi-Z-source Inverters**: These inverters offer lower component ratings and continuous input current, making them suitable for cost-effective and efficient grid-connected applications [47].

- **Transformerless Topologies**: Designed to reduce leakage current, these topologies are effective in improving power efficiency and reliability in grid-tied systems [48].

Ensuring efficient grid connection of QZSIs is critical for the stability and reliability of power systems:

- **Leakage Current Reduction**: Transformerless QZSI designs focus on minimizing high-frequency components in common-mode voltage, effectively reducing leakage current in grid-tied applications [49].
- **Dynamic Response and Harmonic Suppression**: Techniques such as space vector modulation and active power decoupling have been developed to enhance dynamic performance and reduce harmonic distortions in grid-connected systems [50].

2.7. Identification of gaps in the existing literature

The current body of research on QZSI, single-phase inverters, and their grid connections highlights significant advancements and various applications. However, there remain several gaps that warrant further investigation:

While there have been studies on reducing the size and cost of components in QZSIs, such as minimizing the impedance network, further research is needed to develop more cost-effective and compact solutions. This includes optimizing the design to reduce the size of inductors and capacitors without compromising performance [51].

Dynamic performance and stability of QZSI-based systems, especially under varying grid conditions, need more in-depth analysis. The transient interactions and potential instabilities in QZSI-based PV power systems are not well understood and require comprehensive modeling and simulation [52]. These identified gaps present opportunities for further research to enhance the efficiency, reliability, and applicability of QZSI technology in modern power systems.

3. MATERIALS AND METHODS

3.1. Power Circuit Design

Boost capabilities in a single stage of Quasi-Z Source Inverters (QZSIs) is achieved through a unique impedance network composed of inductors and capacitors, which allows for continuous input current and enhanced reliability compared to traditional voltage-source and current-source inverters [53]. The QZSI is particularly advantageous in applications involving renewable energy sources such as fuel cells, where the input voltage can vary significantly [54].

The circuit described in this study is a comprehensive power conversion system that integrates a Fuel Cell stack, a Quasi-Z Source stage, a 3-Level 5-Switch inverter stage, an LCL filter, a variable load configuration, and finally, the grid connection stage. The stages have been presented in Figure 3.1.

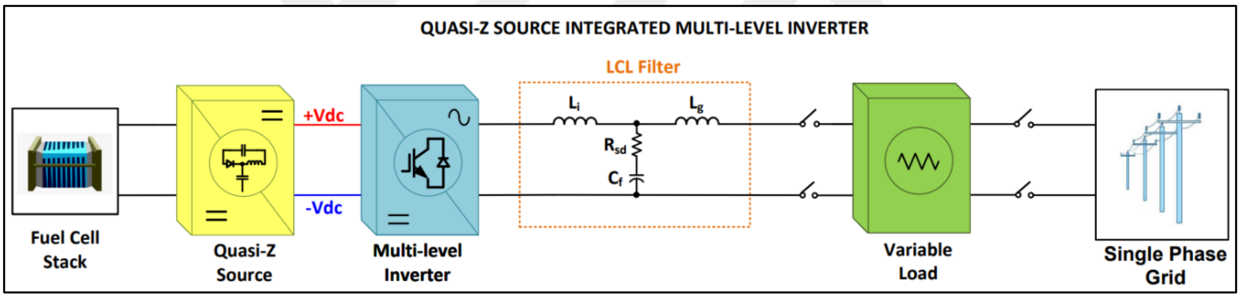

Figure 3.1. Representation of the Stages of the Power Circuit

The first stage of the circuit is the Fuel Cell stack, which serves as the primary source of DC power. Fuel cells generate electricity through an electrochemical reaction between hydrogen and oxygen, producing DC power with water and heat as byproducts. The fuel cell stack is designed to provide a stable and continuous DC output, which is essential for subsequent stages of the power conversion process.

Following the fuel cell stack is the Quasi-Z Source (QZS) stage. The QZS network plays a critical role in boosting and conditioning the DC voltage from the fuel cell stack. It consists of passive components such as inductors and capacitors arranged in a unique configuration that allows for voltage boosting, energy storage, and improved conversion efficiency. The QZS stage also provides short-circuit protection and enhances the overall reliability of the system by mitigating the effects of transient disturbances.

Next, the boosted DC voltage is fed into the 3-Level 5-Switch Inverter stage. This inverter stage is responsible for converting the DC voltage into a high-quality AC voltage suitable for grid connection and load supply. The 3-level inverter topology reduces the total harmonic distortion (THD) of the output waveform, thereby improving power quality. It achieves this by generating multiple voltage levels through a combination of switches and capacitors, resulting in a closer approximation to a sinusoidal waveform compared to traditional inverters.

The AC output from the inverter then passes through an LCL filter, which is composed of a capacitor, resistor and inductors configured to filter out high-frequency harmonics and smooth the AC waveform. The LCL filter ensures that the inverter's output meets the required power quality standards for grid connection, reducing electromagnetic interference (EMI) and protecting sensitive equipment connected to the grid.

Subsequently, the filtered AC power is routed to the variable load configuration. This stage allows for the connection of different types of loads to the system, simulating various real-world scenarios. By adjusting the load, the system's performance under different operating conditions can be analyzed, providing valuable insights into its efficiency, stability, and adaptability.

Finally, the system interfaces with the grid through the grid connection stage. This stage includes switches, synchronization mechanisms, and measuring devices that ensure safe integration with the utility grid. The grid connection stage allows excess power generated by the fuel cell to be fed into the grid, while also enabling the system to draw power rom the grid when needed.

This setup is designed to efficiently convert and manage power from the fuel cell to the grid and various loads. The entire power circuit, including the fuel cell and grid integration, is depicted in Figure 3.2.

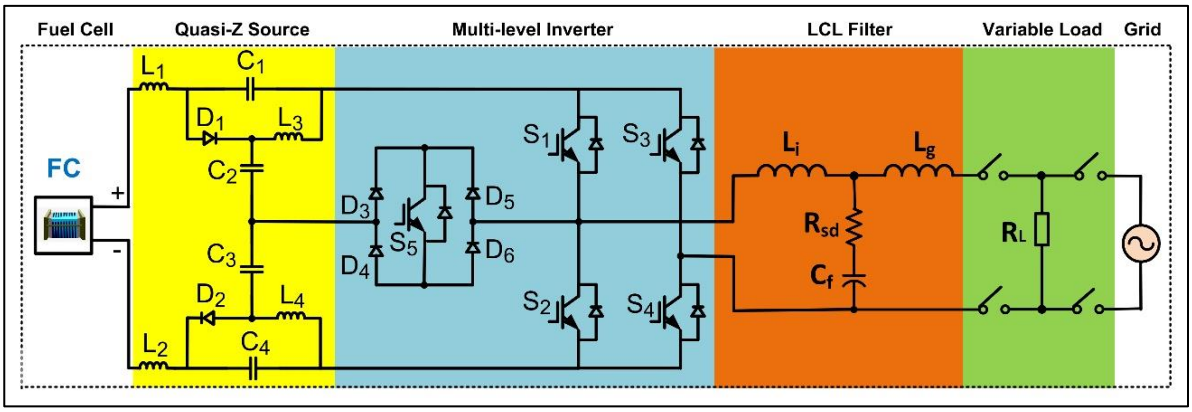

Figure 3.2. Power Circuit Main Stages

3.1.1. Details of the Quasi-Z Source Stage

The Quasi-Z Source Inverter model consists of an impedance network with two inductors and two capacitors configured to enable voltage boost operation. The inverter operates in two primary states: the shoot-through state and the non-shoot-through state. In the shoot-through state, both switches of a phase leg are turned on, allowing energy to be stored in the inductors and capacitors, which is then released during the non-shoot-through state to boost the output voltage [55]. The mathematical model includes detailed equations for these states to ensure accurate simulation results [56].

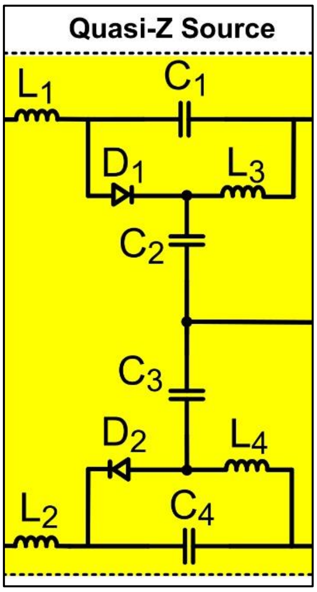

Figure 3.3. QZS Stage

In the design of the Quasi-Z source inverter, key components such as *capacitors* (C_1, C_2, C_3, C_4), *inductors* (L_1, L_2, L_3, L_4), and diodes are used. The values of these components are selected based on the required voltage boost, current handling capability, and desired efficiency. The input voltage (Vin) provided, is expected to fluctuate around 250V with variations between 200V and 250V. For the purpose of calculations, an average input voltage (Vin) of 250V is assumed.

Given the desired output voltage (V_{DC}) of 380V and a nominal modulation index (M) of 0.12, the voltage gain (Gv) is determined as follows:

$$G_v = \frac{V_{dc}}{V_{in}} = \frac{380}{250} = 1.52 \quad (10)$$

The duty cycle (D) is the parameter that controls the amount of time the switch is on relative to the total switching period. It is related to the modulation index (M), which represents the ratio of the peak AC voltage to the peak DC voltage. This relationship can be expressed as:

$$D = 1 - M = 1 - 0.12 = 0.88 \quad (11)$$

The voltage across the capacitors (V_C) is calculated using:

$$V_C = \frac{V_{in}}{2D-1} = \frac{250}{2\times0.88-1} = \frac{250}{0.76} \approx 329V \quad (12)$$

The current through the inductors (I_L) is given by:

$$I_L = \frac{I_{out}}{1-D} = \frac{16}{0.12} \approx 133.33A \quad (13)$$

This indicates the peak current that the inductors must handle. To ensure proper operation, the ratings for the diodes, inductors, and capacitors must be adequate. The diodes must handle a peak inverse voltage (P_{IV}) greater than 380V. The inductors must be capable of handling peak currents of approximately 133.33A and be sized to prevent saturation. The capacitors must be able to handle peak voltages of around 329V and have sufficient capacitance to minimize voltage ripple.

The capacitance *C* required to minimize voltage ripple can be estimated by:

$$C = \frac{I_{out} \times D}{\Delta V \times f_s} \tag{14}$$

where ΔV is the allowable voltage ripple, and f_s is the switching frequency. Assuming an allowable voltage ripple of 1% of the output voltage (3.8V):

$$C = \frac{16 \times 0.88}{3.8 \times 10^4} \approx 370 \mu F \tag{15}$$

The inductance *L* needed to limit current ripple can be estimated by:

$$L = \frac{V_{in} \times D}{\Delta I \times f_s} \tag{16}$$

where ΔI is the allowable current ripple. Assuming an allowable current ripple of 10% of the output current (1.6A):

$$L = \frac{250 \times 0.88}{1.6 \times 10^4} \approx 13.75 mH \tag{17}$$

The design of the Quasi-Z source inverter involves the careful selection of inductors and capacitors to achieve the desired voltage boost and efficiency. The provided equations aid in determining the appropriate component values to ensure reliable operation of the inverter.

During the shoot-through state, both switches are turned on, allowing energy to be stored in the inductors L_1 and L_2, while capacitors C_1 and C_2 provide voltage boosting. The relations for voltages during the shoot-through state are given by:

$$V_{L1} = V_{in} + V_{C2} \tag{18}$$

$$V_{L2} = V_{C1} \tag{19}$$

$$V_{DC} = 0 \tag{20}$$

In the non-shoot-through state, the inductors discharge their stored energy to the capacitors, and the following voltage relations hold:

$$V_{L1} = V_{in} - V_{C1} \tag{21}$$

$$V_{L2} = -V_{C2} \tag{22}$$

$$V_{DC} = V_{C1} + V_{C2} \tag{23}$$

The voltages across the capacitors C_1 and C_2 are determined by the duty cycle D of the shoot-through state, calculated as:

$$V_{C1} = \frac{T_1}{T_1 - T_0} \times V_{in} \tag{24}$$

$$V_{C2} = \frac{T_0}{T_1 - T_0} \times V_{in} \tag{25}$$

Where T_0 and T_1 are the durations of the shoot-through and non-shoot-through states, respectively. The output DC voltage is then given by:

$$V_{DC} = \frac{V_{in}}{1 - 2D} \tag{26}$$

These equations are adapted to reflect the specific characteristics and design of the QZSI system, based on the general principles outlined in the reference literature.

3.1.2. Details of the 5 Switch Inverter Stage

The design and implementation of a five-switch multilevel inverter are elaborated upon in this section. The primary goal of this inverter model is to convert a $380V_{DC}$ input to a $230V_{rmsAC}$ output suitable for grid applications, with a maximum output current of 35A, limited by the fuel cell power capabilities. The design employs MOSFETs as the switching elements, utilizing a high-frequency PWM technique to achieve high efficiency and low harmonic distortion.

The inverter is designed with specific operational parameters in mind. The input voltage is maintained at $380V_{DC}$, while the desired output voltage is $230V_{rmsAC}$. The inverter is capable of delivering a maximum output current of 35A, with a switching frequency set at 10kHz. A modulation index of 0.12 is employed to ensure the precise control of the output waveform.

The schematic diagram of the five-switch multilevel inverter illustrates the circuit configuration, where five MOSFETs (S_1, S_2, S_3, S_4, S_5) are utilized as the primary switching elements. Each MOSFET block is paired internally with a corresponding diode to prevent reverse current and ensure the proper functioning of the inverter. This arrangement allows the generation of multiple voltage levels, which is crucial in reducing harmonic distortion in the output waveform.

The operational principle of the inverter revolves around producing five distinct voltage levels: V_{DC}, $V_{DC/2}$, 0, -$V_{DC/2}$, and -V_{DC}. These voltage levels are achieved by controlling the states of the MOSFETs in a specific switching sequence. The use of high-frequency PWM is integral to this process, as it allows for precise modulation of the switching elements, thereby achieving the desired output voltage and minimizing harmonics.

This inverter is classified as a five-level inverter, which is a type of multilevel inverter. Specifically, this inverter can be identified as a NPC inverter. NPC inverters are known for their ability to produce multiple voltage levels with reduced harmonic distortion and improved voltage quality.

The design process for the inverter begins with the calculation of the DC link voltage. This voltage must be sufficient to generate the desired AC output voltage of $230V_{rms}$. For a five-level inverter, careful design of V_{DC} is essential to ensure the generation of the required voltage levels. The maximum output current of 35A, corresponding to the $230V_{rmsAC}$ output, necessitates careful design considerations on the AC side to handle this current.

A control block is used to generate the necessary PWM signals. This control block is responsible for managing the switching sequence accurately. The nominal modulation index of 0.12 and the switching frequency of 10kHz are critical parameters in this design, ensuring precise control of the inverter.

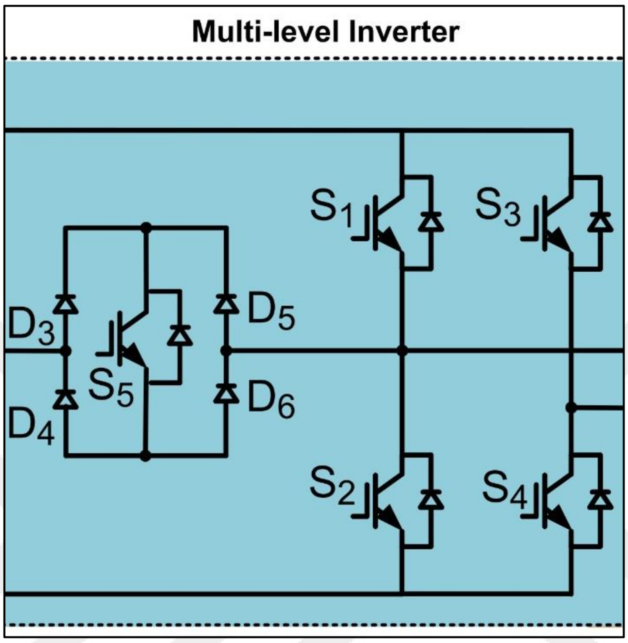

Figure 3.4. 5-Switch Inverter Stage.

3.1.3. LCL Filter Design

An LCL filter is incorporated into the design to enhance the quality of the output power and minimize harmonic distortion, thus ensuring a smooth sinusoidal output. The LCL filter consists of two inductors (L_i and L_g), a capacitor (C_f), and a damping resistor (R_{sd}). The primary function of the LCL filter is to attenuate the high-frequency harmonics generated by the switching actions of the inverter.

The design process of the LCL filter involves selecting appropriate values for the inductors and capacitor to achieve the desired attenuation while maintaining stability. The inductance values (L_i and L_g) are chosen based on the desired cutoff frequency and the impedance matching requirements. The capacitor (C_f) is selected to provide the necessary reactive power support and to set the filter's resonant frequency.

From the literature, it is suggested that the cutoff frequency for LCL filters in grid-connected inverters should be around one-tenth of the switching frequency. Given a switching frequency (fs) of 10 kHz, the cutoff frequency (fc) can be set to approximately 1 kHz [57],[58]. The resonant frequency (fr) of the LCL filter is determined by the equation:

$$f_r = \frac{1}{2\pi\sqrt{(L1+L2)\times Cf}} \tag{27}$$

Assuming the total inductance is equally split between the inverter-side and grid-side inductors, the total inductance (L_{total}) required to achieve the desired cutoff frequency can be determined. Given the desired resonant frequency (fr) is 1,000 Hz and an assumed initial total inductance:

$$L_{\text{total}} = 2 \times 4\text{ mH} = 8\text{ mH} \tag{28}$$

This value is chosen to provide adequate filtering without causing significant voltage drop or excessive size. Using the resonant frequency formula to solve for the capacitance (C_f):

$$C_f = \frac{1}{(2\pi f_r)^2(L1+L2)} \tag{29}$$

Substituting the values:

$$C_f = \frac{1}{(2\pi\times 1{,}000)^2\times 8\times 10^{-3}} \approx 3.18\ \mu F \tag{30}$$

To ensure that the inductor values are within practical limits and provide the desired filtering, the inductance values should be recalculated if necessary:

$$L_i = L_g = \frac{8\text{ mH}}{2} = 4\text{ mH} \tag{31}$$

The damping resistor (R_{sd}) is included to dampen the resonance peak and improve the filter's stability. The value of R is typically chosen to be a fraction of the characteristic impedance of the LC circuit. The characteristic impedance (Zc) can be calculated as:

$$Z_c = \sqrt{\frac{L_{\text{total}}}{C}} \tag{32}$$

Substituting the given values:

$$Z_c = \sqrt{\frac{8\times10^{-3}}{3.18\times10^{-6}} \approx 50.23\Omega} \tag{33}$$

The damping resistor R is then chosen to be a fraction of this value. Assuming a damping factor of 0.1:

$$R_{sd} = 0.1 \times Z_c \approx 5\Omega \tag{34}$$

The LCL filter stage is meticulously designed to attenuate high-frequency harmonics and enhance output power quality. The careful selection of inductors, capacitors, and a damping resistor ensures the effective operation and stability of the filter, thereby improving the overall performance of the NPC inverter system. The calculations, based on literature recommendations, provide a robust basis for the implementation of the LCL filter.

3.1.4. Configuration of the Fuel Cell as the DC Source

The fuel cell is configured as the primary DC source for the QZSI. A hydrogen fuel cell model is used, providing a stable DC voltage output. The fuel cell model is used as a already integrated model from the Simulink environment, where its dynamic characteristics, such as voltage output can be adjusted. The model also accounts for the effects of hydrogen consumption and temperature variations on the output voltage, ensuring accurate real-world operating conditions.

Advanced FC control techniques may incorporate algorithms such as Maximum Power Point Tracking (MPPT) to extract the maximum possible power from the fuel cell, especially in applications where the fuel cell operates under varying environmental conditions.

MPPT control technic has not been utilized in this study. Instead of a DC-DC controller, the QZS stage boost the DC voltage to the optimum operating range. Additionally, the fuel cell model operates within its safe operating limits, preventing issues such as overloading.

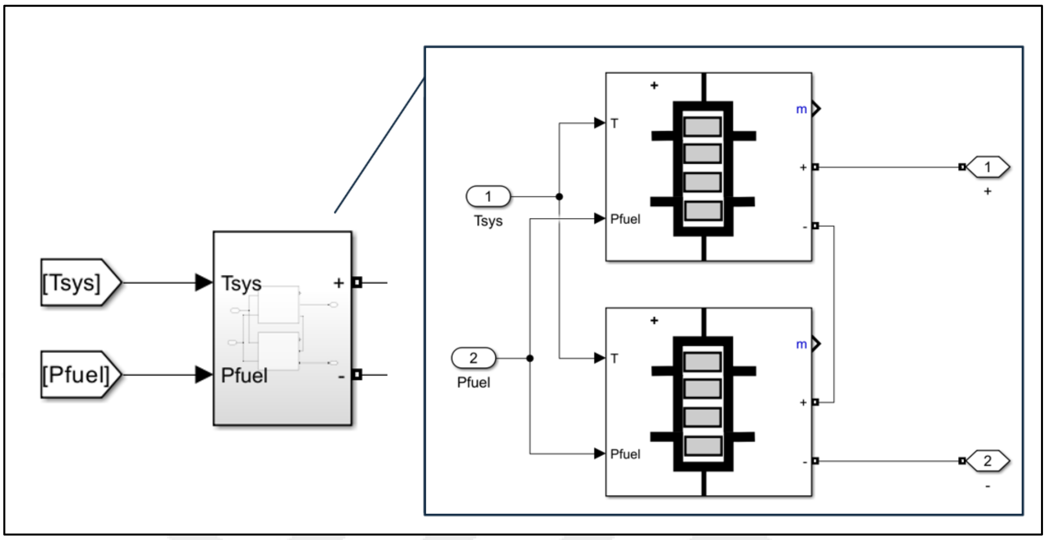

Figure 3.5. Fuel Cell Stacks.

The fuel cell stack has 2 fuel cell blocks that are connected in series to achieve the desired input DC voltage range. The preset model of "SOFC - 3 kW - 100 V_{DC}" has been used with the parameters given in Table 3.1.

Table 3.1. Fuel Cell Parameters.

Parameter	Value
Preset model	SOFC - 3 kW - 100 *VDC*
Model detail Level	Detailed
Voltage at 0A and 1A [V_0(V), V_1(V)]	[141.34, 133]
Nominal operating point [Inom(A), Vnom(V)]	[30, 106.5]
Maximum operating point [Iend(A), Vend(V)]	[33.2, 104.86]
Number of cells	119
Nominal stack efficiency (%)	52
Operating temperature (Celsius)	600
Nominal Air flow rate (lpm)	635
Nominal supply pressure [Fuel (bar), Air (bar)]	[1.35, 1]
Nominal composition (%) [H2 O2 H2O(Air)]	[50, 21, 3]

3.1.5. Grid Synchronization and Connection

The grid synchronization process was simulated to demonstrate the inverter's capability to connect and interact with the grid. Phase-locked loop (PLL) was employed to synchronize the inverter's output with the grid's voltage and frequency. The simulation included scenarios of both grid-tied and islanded operation modes, highlighting the inverter's flexibility in different operational contexts.

The dq transformation is a mathematical technique used to simplify the control of three-phase power systems by transforming the three-phase currents and voltages into a rotating reference frame. This transformation decouples the active and reactive power components, facilitating easier control of grid-connected inverters under unbalanced conditions. In QZSI-based systems, maintaining stability and efficiency in the dq frame is critical, particularly during events such as voltage sags or harmonic distortions. Proper control strategies ensure that the inverters can inject stable and smooth power into the grid, even under fluctuating input conditions [59].

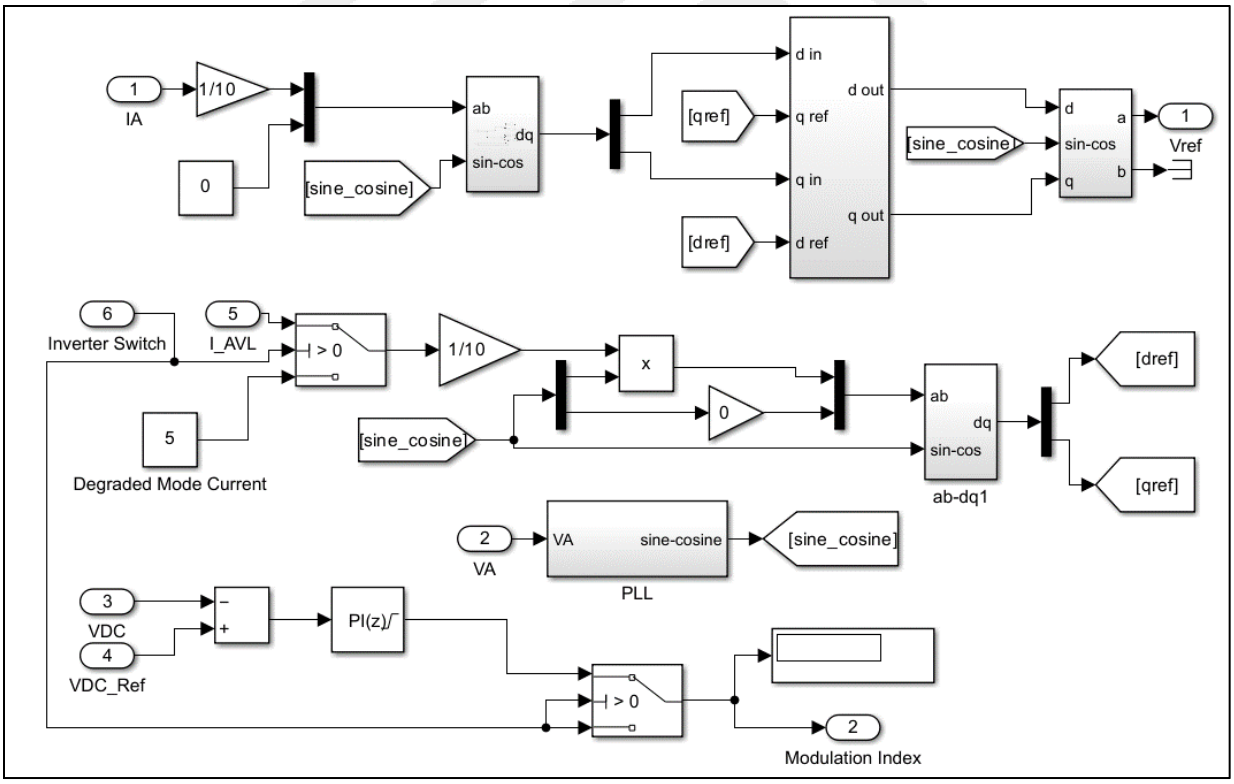

Figure 3.6. Unbalanced DQ conversion and modulation index control.

3.2. Mathematical Modeling of the Power Circuit

The mathematical modeling of a 5-switch NPC QZSI involves developing state-space equations that describe the dynamics of the system. This includes modeling the inductor currents and capacitor voltages, which are influenced by the shoot-through duty cycle and modulation index. The 5-switch NPC QZSI topology reduces the number of switches required while maintaining effective control over the output voltage and current.

The steady-state and transient analyses of this topology are essential for ensuring balanced neutral points and stable operation under varying load conditions [60].

3.3. Principles of Operation

The operation of QZSIs involves two main states: the active state and the shoot-through state. During the active state, the inverter functions like a traditional inverter, delivering power to the load. In the shoot-through state, both switches of a phase leg are turned on simultaneously, allowing energy to be stored in the inductors and capacitors of the impedance network. This stored energy is then used to boost the output voltage when the inverter returns to the active state. This shoot-through capability is crucial for achieving voltage boost without the risk of damaging the inverter, making QZSIs highly efficient for variable input voltage conditions [61].

3.3.1. Operation States

The operation of Quasi-Z Source Inverters (QZSIs) is characterized by two distinct states, the active state and the shoot-through state. In the active state, the QZSI operates similarly to a conventional inverter, with power being delivered to the load. During this state, the inverter switches function normally, directing energy flow from the input to the output, ensuring efficient power conversion.

When the $+V_{DC}$ state is engaged, switches S_1 and S_4 are activated. During this state, energy is directed from the DC source to the load, resulting in a positive output voltage equal to the DC input voltage.

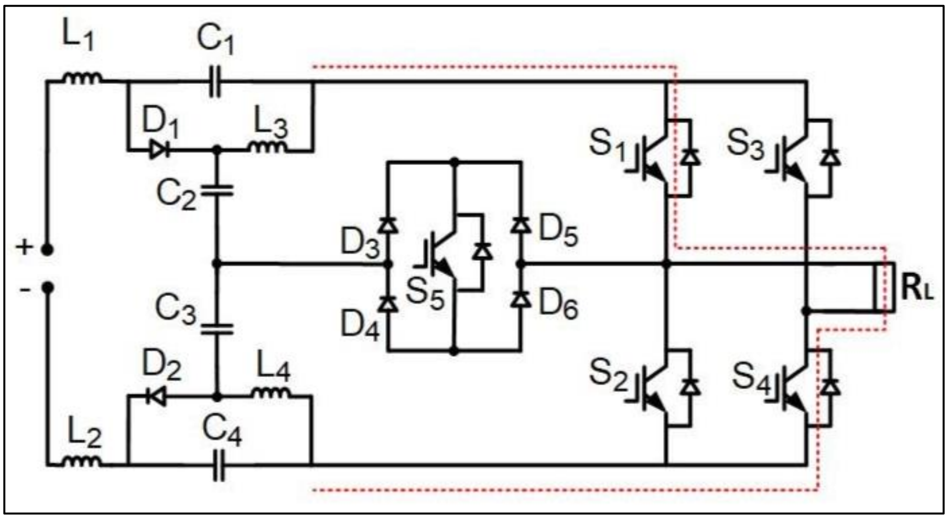

Figure 3.7. $+V_{DC}$ state flow.

During the $+V_{DC/2}$ state, switches S_4 and S_5 are activated. This configuration allows the output voltage to be reduced to half of the DC input voltage.

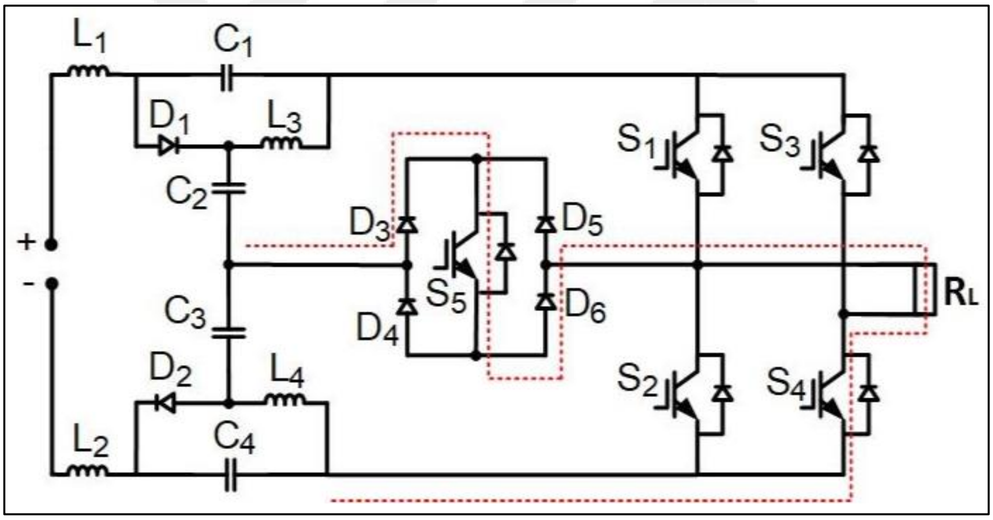

Figure 3.8. $+V_{DC/2}$ state flow.

In the Neutral state, all switches are deactivated. Consequently, no energy is delivered to the load, resulting in zero output voltage.

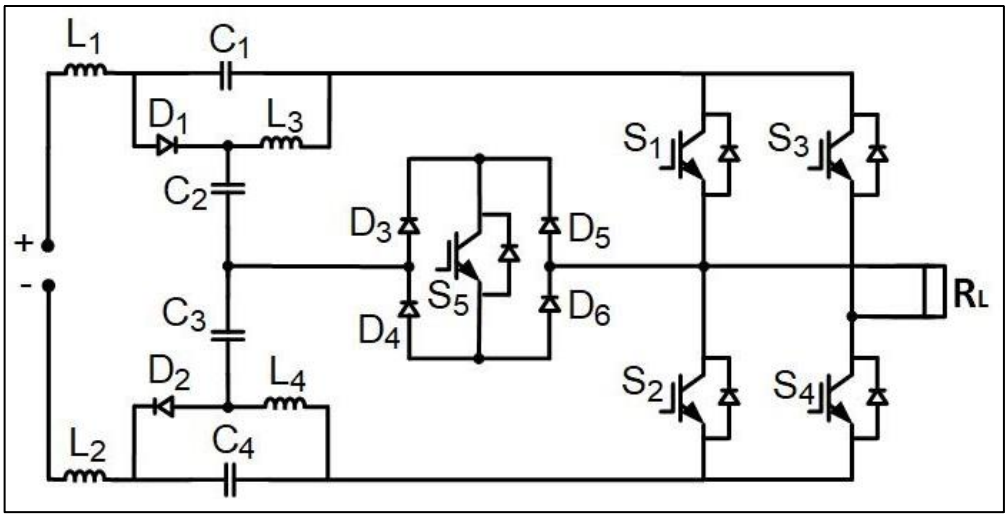

Figure 3.9. Neutral state flow.

For the -VDC state, switches S_2 and S_3 are activated. Energy is directed in the opposite direction during this state, producing a negative output voltage equal to half of the DC input voltage.

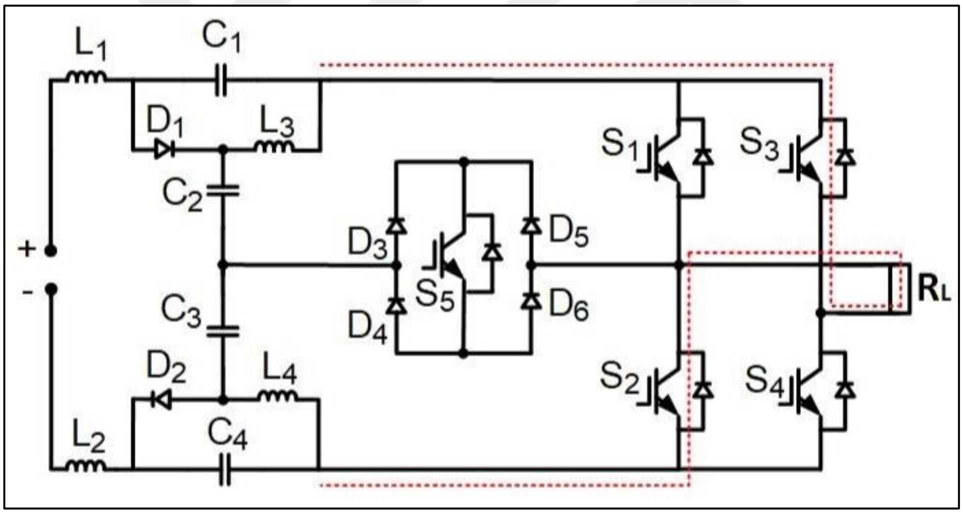

Figure 3.10. -V_{DC} state flow.

When the -$V_{DC/2}$ state is engaged, switches S_3 and S_5 are activated. The output voltage is rendered negative and is reduced to half of the DC input voltage.

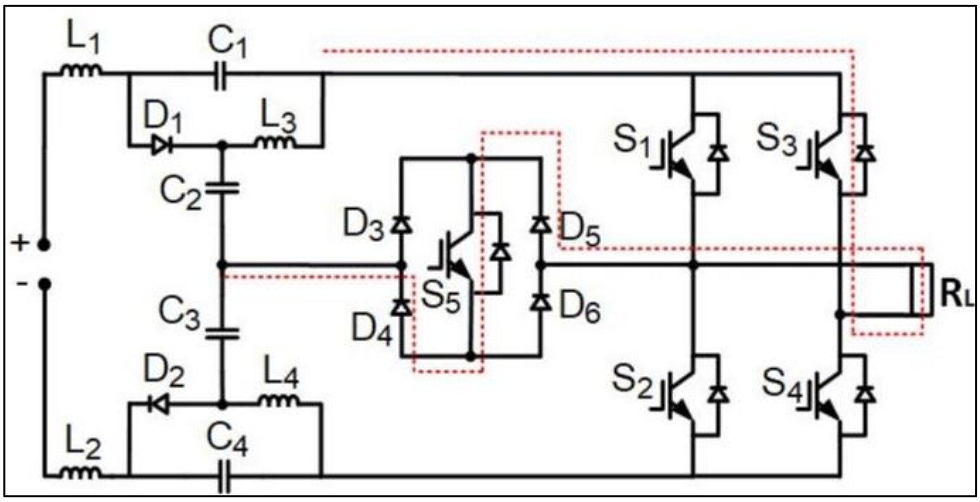

Figure 3.11. -$V_{DC/2}$ state flow.

The shoot-through state is a unique feature of QZSIs, where both switches of a phase leg are turned on simultaneously. This allows energy to be stored within the inductors and capacitors of the impedance network. The energy accumulated in the passive components during this state is crucial for the voltage-boosting capability of the QZSI. In this state, switches S1 and S3 are simultaneously activated. Energy is stored in the Quasi-Z network by allowing both switches in the phase leg to conduct simultaneously.

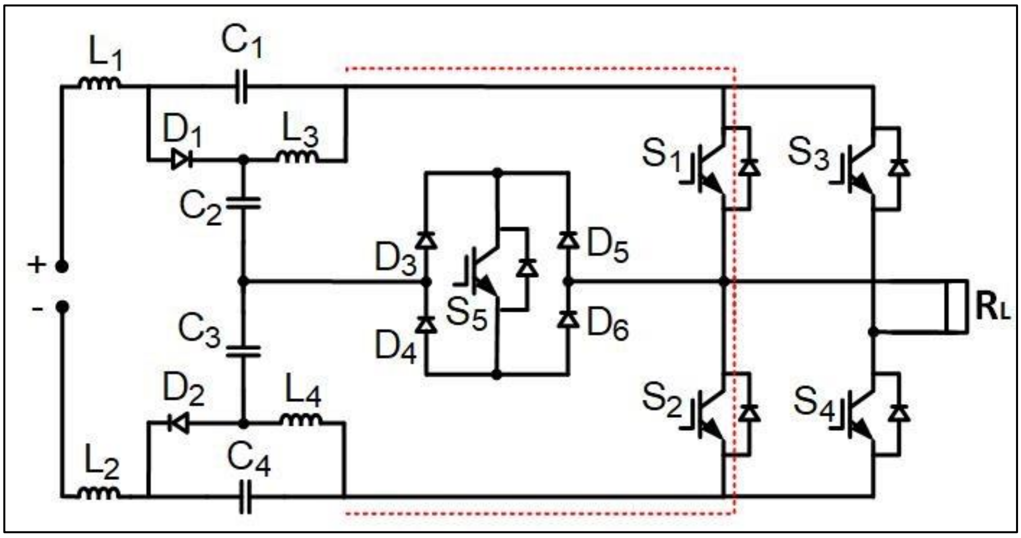

Figure 3.12. Shoot-Through state flow.

Upon returning to the active state, the stored energy is released, providing an increased output voltage. This state significantly enhances the inverter's ability to manage variable input voltage conditions without the risk of damage, thus improving overall efficiency. The unique capability to store and boost energy makes QZSIs highly suitable for applications with variable input voltages.

The transition between the active and shoot-through states is governed by control algorithms that ensure the optimal performance of the QZSI. The timing and duration of these states are controlled to balance energy storage and power delivery, maintaining high efficiency and reliability under varying operational conditions. The operating states with corresponding gate states of the switches and output voltages of the inverter have been presented in Table3.2.

Table 3.2. Operating States.

State	G1	G2	G3	G4	G5	Output Voltage (V)
+V_{DC}	1	0	0	1	0	$+V_{DC}$
+$V_{DC/2}$	0	0	0	1	1	$+V_{DC/2}$
0 (Neutral)	0	0	0	0	0	0
-V_{DC}	0	1	1	0	0	$-V_{DC/2}$
-$V_{DC/2}$	0	0	1	0	1	$-V_{DC}$
Shoot-Through	1	0	1	0	0	0

3.3.2. Bi-Directional Operation

The bi-directional operation of QZSIs is essential for applications requiring power flow in both directions, such as electric vehicles and energy storage systems. This capability allows the QZSI to manage both charging and discharging processes efficiently, making it highly suitable for renewable energy systems and grid integration.

The QZSI operates in two main modes during bi-directional operation: the buck mode and the boost mode. In the buck mode, the QZSI steps down the voltage to charge the energy storage system, such as a supercapacitor or battery. Conversely, in the boost mode, the QZSI steps up the voltage to supply power from the DC supply system to the load or the grid [62]. This dual capability is achieved by the unique impedance network of the QZSI, which allows continuous current flow and voltage boost or buck operations as needed [63].

In electric vehicle applications, the bi-directional QZSI can enhance the overall efficiency and reliability of the powertrain by enabling seamless transitions between driving and regenerative braking modes. The ability to handle power flow in both directions not only improves energy efficiency but also extends the lifespan of the energy storage components by maintaining optimal charge and discharge cycles [64].

Additionally, the bi-directional QZSI is capable of mitigating the input current ripples, which is critical for maintaining the stability of the power system. This is particularly important in grid-tied applications where fluctuating power demands can lead to instability if not properly managed [65].

Overall, the bi-directional operation of QZSIs provides a versatile and efficient solution for modern power systems, enabling better integration of renewable energy sources and enhancing the performance of electric vehicles and energy storage systems. The continuous research and development in this area aim to further optimize the design and control strategies, ensuring that QZSIs can meet the increasing demands of advanced power applications [66].

3.4. Control Methods

The simulation setup for the QZSI model is constructed using MATLAB/Simulink. Simulink is selected due to its powerful capabilities in modeling, simulating, and analyzing dynamic systems, particularly in power electronics. The setup includes modeling the QZSI using standard Simulink blocks such as voltage sources, switches, inductors, and capacitors. The simulation employs the SPWM technique with 2 carrier signals to control the switching of the inverter with multiple voltage levels, which improves the performance and reduces harmonic distortion [67].

3.4.1. Modulation and Signal Generation

The modulation process in the described system is achieved through Sinusoidal Pulse Width Modulation (SPWM) utilizing two distinct carrier signals, C_a and C_b. The reference voltage (V_{ref}) is produced based on the feedback from the current controller. This controller is responsible for maintaining the desired current. Concurrently, the DQ transformation is employed to decouple the active and reactive power components, which simplifies the control of the grid-connected inverter, particularly because of the single phase application. This decoupling allows for more straightforward management of the inverter's output, ensuring stability and efficiency.

Within the modulation process, the generated V_{ref} is compared against the two carrier signals, C_a and C_b, to determine the switching states of the inverter. The outputs from these comparisons are processed through logical blocks to generate preliminary signals, denoted as *PG1* through *PG5*. These logical operations include a series of comparisons and subsequent AND/OR operations. The SPWM modulation with two carrier signals enhances the precision of the modulation process. The logical operations performed on the intermediate signals involve specific comparisons, which are depicted in the block diagrams.

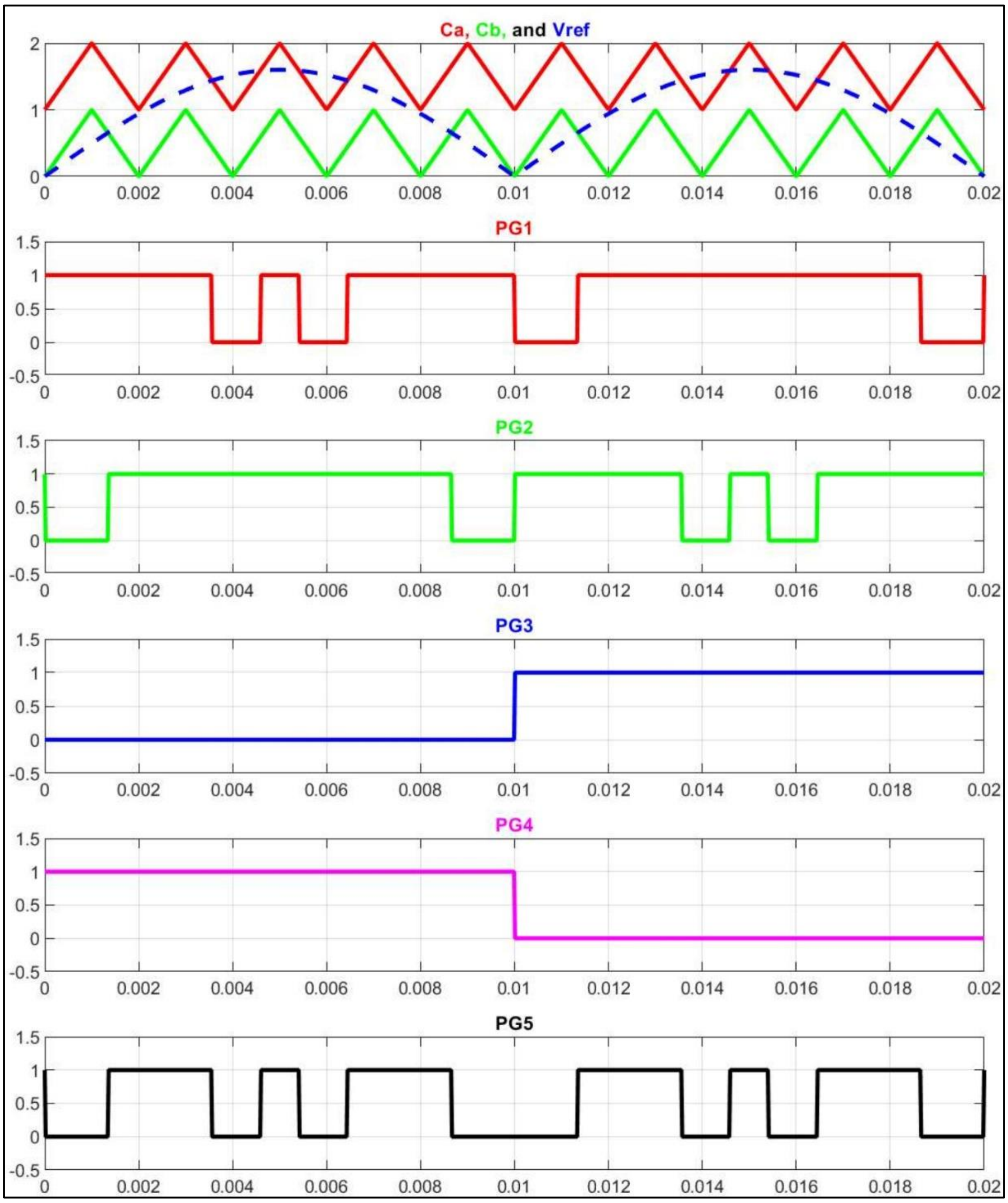

Figure 3.13. Level shifted SPWM method.

The modulation comparison outputs are then translated into the actual gating signals for the five-power semiconductor switching devices, using simple combinational logical expressions, which are shown below:

$$PG1 = (Ca \geq absVref \wedge Vref \geq 0) \vee (Cb \leq absVref \wedge Vref \leq 0) \tag{35}$$

$$PG2 = (Ca \geq absVref \wedge Vref \leq 0) \vee (Cb \leq absVref \wedge Vref \geq 0) \tag{36}$$

$$PG3 = Vref < 0 \quad (37)$$

$$PG4 = Vref \geq 0 \quad (38)$$

$$PG5 = absVref \leq Ca \wedge absVref \geq Cb \quad (39)$$

The preliminary signals, *PG1* and *PG2*, are then compared with modulation index to produce the gate signals, *G1* through *G2*. The rest of the gate signals have been carried over from preliminary gate signals directly. This process is designed to meet the desired output voltage and current requirements, thereby optimizing the inverter's performance.

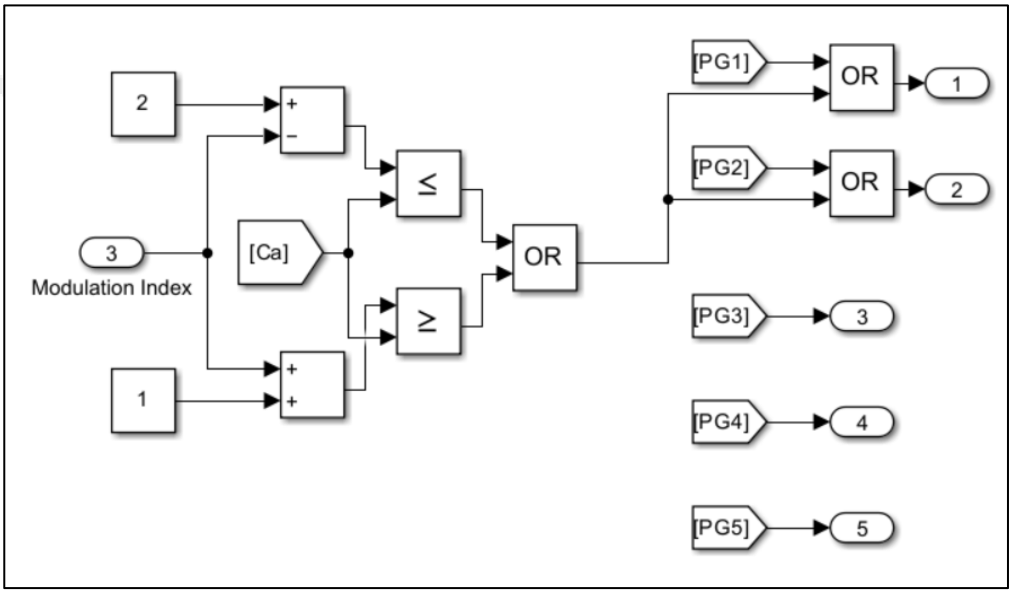

Figure 3.14. Modulation index comparison within the modulation outputs.

3.4.2. Current Control

Current control in QZSIs is crucial for maintaining the stability and performance of the system. The primary objective of current control is to regulate the output current to match the desired reference value, ensuring efficient power delivery and minimizing harmonic distortion.

The current control strategy typically involves the implementation of a PI controller with the DQ transform of the grid connection. After the unbalanced DQ transformation, the reference voltage is created to feed into the modulation controller to create the required gate signals of the transistors.

The controller continuously adjusts the switching states of the inverter to achieve the desired current waveform. The PI controller operates by minimizing the error between the reference current and the actual output current.

In QZSI applications, current control is particularly important due to the presence of the impedance network, which affects the dynamics of the system. The control algorithm must account for the interactions between the inductors and capacitors in the Quasi-Z source network, ensuring stable operation and effective power conversion. Proper tuning of the current controller parameters is essential to achieve fast transient response, low THD, and robust performance under varying load and grid conditions.

3.4.3. DC Link Control

DC link control in QZSIs is essential for maintaining a stable DC link voltage, which directly influences the performance and efficiency of the inverter. The DC link voltage must be regulated to ensure proper power conversion and to prevent voltage fluctuations that could affect the stability of the system.

The DC link control strategy involves monitoring the DC link voltage and adjusting the shoot-through modulation index to regulate the voltage levels. The control system uses a feedback loop, where the measured DC link voltage is compared to a reference value, and the error is processed by a PI controller.

The PI controller for the DC-link voltage was tuned using a modified Ziegler-Nichols method, adapted to suit the specific dynamics of the QZSI system. This involved first determining the ultimate gain K_U and oscillation period P_U, and then using these values to calculate the controller parameters:

$$K_P = 0.45\, K_U \tag{40}$$

$$K_i = \frac{K_P}{1.2\, P_u} \tag{41}$$

The output of the controller determines the shoot-through modulation index, which in turn affects the energy storage and release in the Quasi-Z source network. The modulation index M, which controls the inverter's output voltage, is determined by the ratio of the desired DC-link voltage V_{DC} to the input voltage V_{in} provided by the fuel cell:

$$M = \frac{V_{DC}}{V_{in}} \tag{42}$$

The PI controller adjusts the modulation index according to the error between the DC link voltage and the set DC link voltage. Set DC link voltage has been determined as 380V according to the tuning of the model and the literature research findings.

Bi-directional DC link control is particularly important in applications where the QZSI is used for energy storage systems or inverters that need to operate in both charging and discharging modes. The control algorithm must ensure seamless transitions between these modes, maintaining the desired DC link voltage under different operating conditions. With the utilization of a PI control for the current control of the inverter, it can pull power from the grid to stabilize the DC link voltage. The inverter acts as a rectifier to transform the AC grid voltage into DC voltage and according to the switching signals provided by the current controller supported by the PI controller, the DC link voltage can be controlled and even be utilized as a DC supply or a charger circuit.

Effective DC link control enhances the overall performance of the QZSI, ensuring stable operation, efficient power conversion, and reliable integration with renewable energy sources and the electrical grid.

3.5. Explanation of the Load Scenarios Tested

In this study, fuel cell rated power is determined as 6000 W. Variable load power is ranging from 1000 W to 8000 W maximum. The mentioned operational modes are described below:

- **Mode 1**: The fuel cell supplies the load and feeds excess power to the grid.

- **Mode 2**: The fuel cell and the grid jointly supply the load.
- **Mode 3**: The grid is off, and the fuel cell alone supplies the load.
- **Mode 4**: The fuel cell is off, and the grid alone supplies the load.

The load scenarios tested in the simulation encompass various operational modes to evaluate the performance of the QZSI with the fuel cell as the DC source. The scenarios are structured as follows:

In Case 1, the QZSI system operates under different modes to illustrate its flexibility and efficiency in managing power flow between the fuel cell, load, and grid.

- **Mode 1 (0 to 1 second):** The fuel cell supplies power to a 1000 W load, with excess power being fed into the grid, demonstrating the system's capability to effectively utilize surplus energy.

- **Mode 2 (1 to 2 seconds):** The load demand increases to 7000 W, necessitating additional power from the grid to supplement the fuel cell's output. This mode highlights the QZSI's robustness in handling higher load demands.

- **Mode 1 (2 to 3 seconds):** The fuel cell operates at a nominal 6000 W, supplying a 2000 W load and feeding an estimated 4000 W of excess power back into the grid, emphasizing the system's efficiency in managing surplus power.

- **Mode 3 (3 to 4 seconds):** The fuel cell alone supplies a 2500 W load, with no interaction with the grid, demonstrating the QZSI's suitability for standalone operations.

In Case 2, the QZSI system continues to display its adaptability and efficiency under various operational conditions.

- **Mode 1 (4 to 5 seconds):** The fuel cell supplies a 3000 W load, with excess power fed into the grid, showcasing the system's ability to support the grid with surplus energy.

- **Mode 2 (5 to 6 seconds):** The load demand increases to 8000 W, requiring an estimated 2000 W from the grid to supplement the fuel cell's output of 6000 W, demonstrating the QZSI's capacity to draw necessary power from the grid under high load conditions.

- **Mode 4 (6 to 7 seconds):** The fuel cell is off, and the grid supplies the entire 2000 W load, illustrating the system's reliability in maintaining continuous power supply using grid power alone.

- **Mode 1 (7 to 8 seconds):** The fuel cell operates at 6000 W, supplying a 2000 W load and feeding an estimated 4000 W of excess power back into the grid, reinforcing the system's efficiency in handling surplus power.

Overall, these case analyses shall illustrate the QZSI system's robust performance in managing varying load demands and power sources, effectively balancing power generation and consumption while ensuring grid stability and reliability. Detailed numerical results and performance metrics will be presented in subsequent sections to provide a comprehensive evaluation of the system's capabilities.

Efficiency for each scenario will be measured and documented, indicating the performance of the QZSI under different load conditions and operational modes. With the simulation model established and the parameters set, the system's performance under different load scenarios will be analyzed. The following section presents the results of these simulations and discusses their implications.

4. ANALYSIS AND DISCUSSION

4.1. MATLAB/Simulink Model and System Parameters

To verify the performance of the proposed Quasi-Z source integrated multi-level inverter (QZS-MLI) topology and the designed controllers, simulation results captured from MATLAB/Simulink software are presented. The effectiveness of the proposed QZS-MLI system is tested with different case studies.

The overall MATLAB/Simulink model of the proposed QZS-MLI system is shown in Figure 4.1. The power circuit design parameters and control parameters used in the simulation model are given in Table 4.3. Control algorithms specified in Chapter 3, are implemented using Simulink blocks and MATLAB code within the MATLAB editor.

In this simulation study, the following features are aimed to be explored through different case studies:

- To observe the steady-state and dynamic response of the system under changing load conditions.
- To monitor power flows between input and output ports in different operating modes, depending on the variations in FC parameters and grid conditions.
- To demonstrate that the voltage imbalance between the lower and upper terminals of the DC link can be successfully compensated.
- Simulation results validate the high efficiency and stability of the QZS-MLI under various load conditions, supporting its use in grid-tied and standalone renewable energy applications.

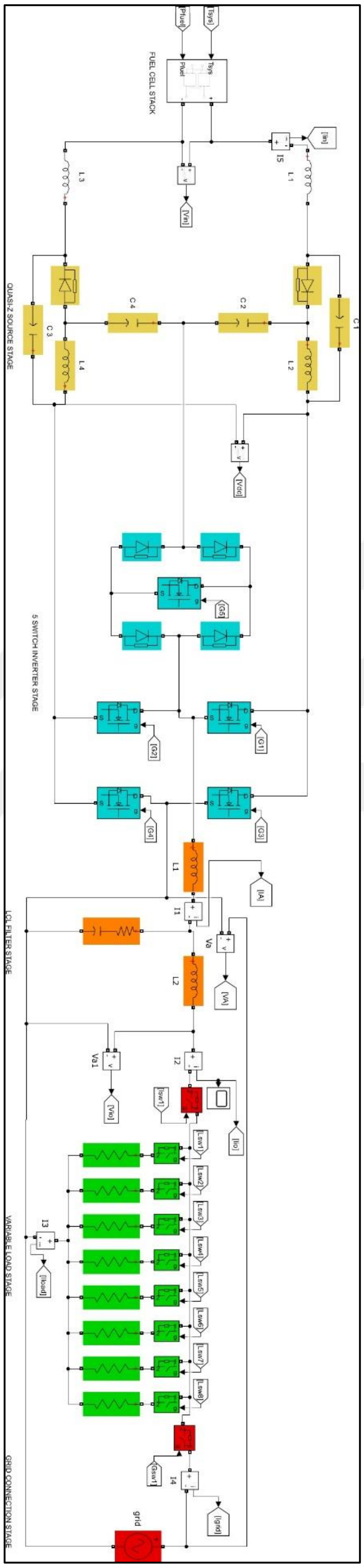

Figure 4.1. FC Integrated Grid Connected Power Circuit Simulink Model.

Table 4.1. MATLAB/Simulink Simulation Parameters.

Solver Maximum Step Size	1e-06 s
Duration of Simulation Time	8 s

Table 4.2. DC-Link PI Control Parameters

Kp	0.0005
Ki	0.01

The system parameters have been optimized according to the simulation results with iterations. The parameters the for the simulation model of the QZS-MLI have been defined and presented in Table 4.3.

Table 4.3. System Parameters of Simulation Model.

System	Parameter	Value
Fuel Cell	Nominal power rating	6000 W
	Nominal operating point (In, Vn)	30.06 A, 213 V
	Open circuit voltage (Voc)	282.68 V
	Maximum operating point (Im, Vm)	33.2 A, 209.72 V
	Number of cells	238
	Types of cells	Solid Oxide FC
	System temperature	873 K
	Nominal supply pressure (Fuel , Air)	1.35 bar, 1 bar
Quasi-Z Source	C1,C2	1 mF
	L1,L2,L3,L4	1 mH
	Nominal Voltage Gain	1.52
	Nominal Modulation Index	0.12
Multilevel Inverter	Rated Maximum Current	35A
	DC Link Voltage	380 V
	Switching Frequency (fs)	10 kHz
LCL Filter	Li	4 mH
	Lg	2.4 mH
	Cf	3 µF
	Rsd	7.5 Ohm
Variable Load	Load Range	1000 - 8000 W
Grid	Voltage	230 V RMS
	Frequency	50 Hz

4.2. Presentation of Simulation Results for Different Load Scenarios

The simulation results for the QZSI were obtained using MATLAB/Simulink, focusing on various load scenarios to evaluate the inverter's performance. The results are presented for each case as follows.

In Case 1, the performance of the QZSI system is evaluated under different operating modes over a period of four seconds. The analysis covers four distinct modes, each demonstrating the system's response to varying load demands and fuel cell power outputs, highlighting the QZSI's capability to manage power flow and maintain grid stability.

During Mode 1, from 0 to 1 second, the fuel cell operates at 5728 W, supplying a load of 1000 W. The excess power of 4453 W is fed into the grid. This scenario illustrates the system's ability to efficiently utilize surplus power generated by the fuel cell and contribute it to the grid, enhancing the overall grid stability and efficiency.

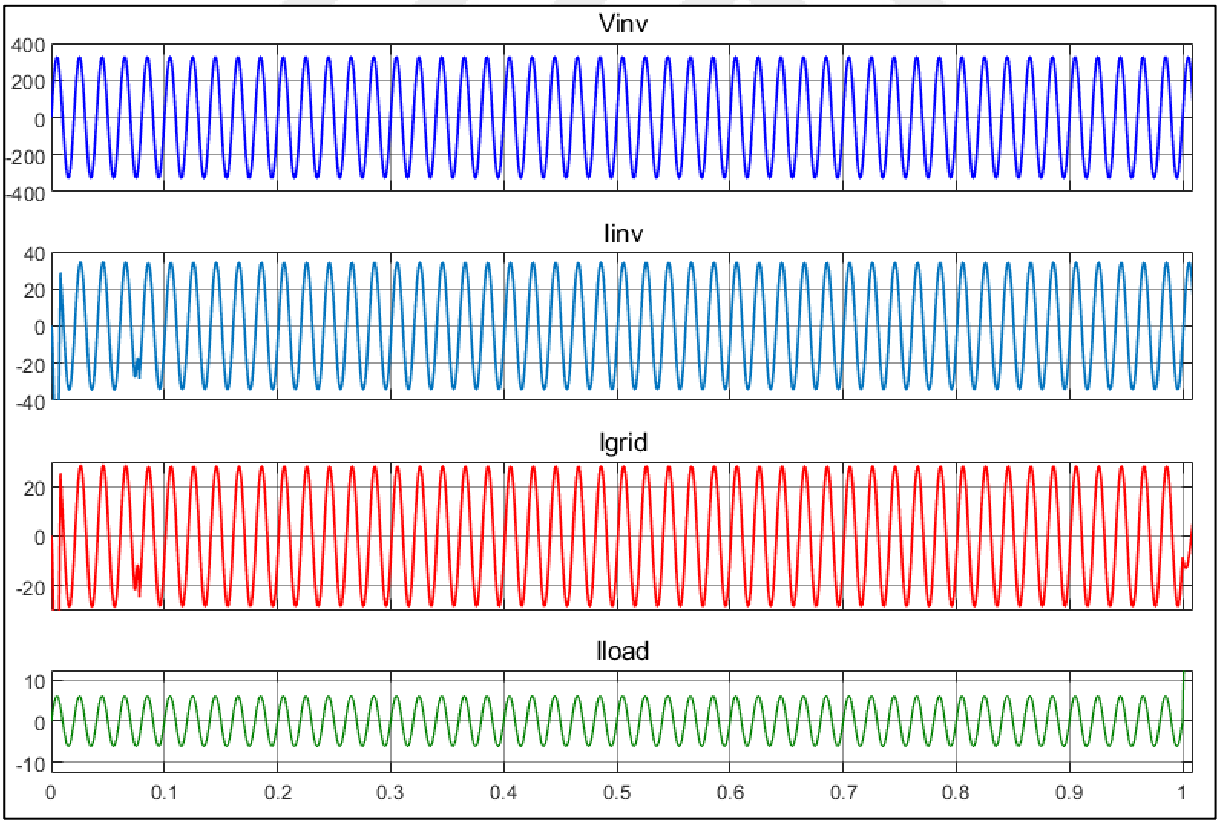

Figure 4.2. Case 1, Mode 1, from 0 to 1 second.

In Mode 2, from 1 to 2 seconds, the fuel cell continues to operate at a slightly higher output of 5749 W, while the load demand increases to 7000 W. This results in a power deficit of 1601 W, which is supplied by the grid. This mode demonstrates the QZSI system's ability to draw additional power from the grid to meet higher load demands, ensuring continuous and reliable power supply to the load.

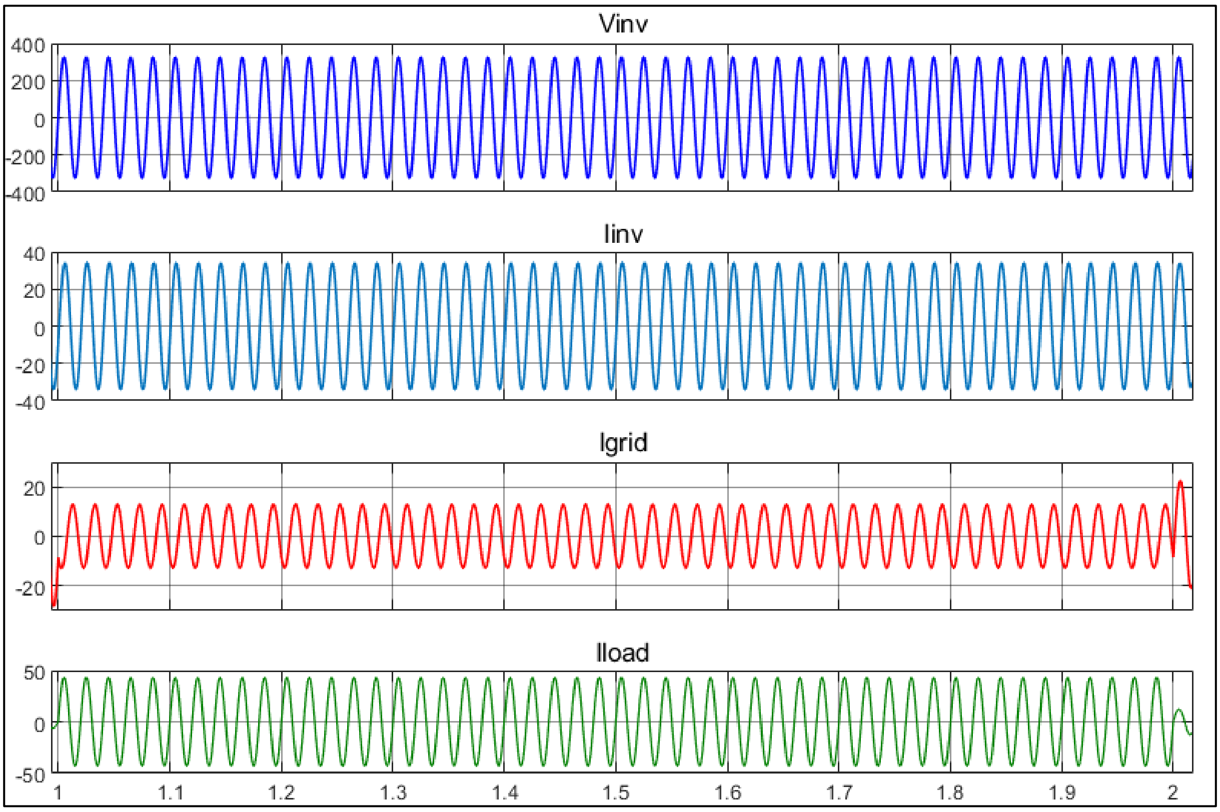

Figure 4.3. Case 1, Mode 2, from 1 to 2 seconds.

Returning to Mode 1 from 2 to 3 seconds, the fuel cell's output increases to 5807 W, and the load demand is adjusted to 2000 W. The system again operates with excess power, feeding 3539 W back into the grid. This scenario further highlights the system's capability to dynamically adjust to changing load conditions and efficiently manage surplus power generation by feeding it into the grid.

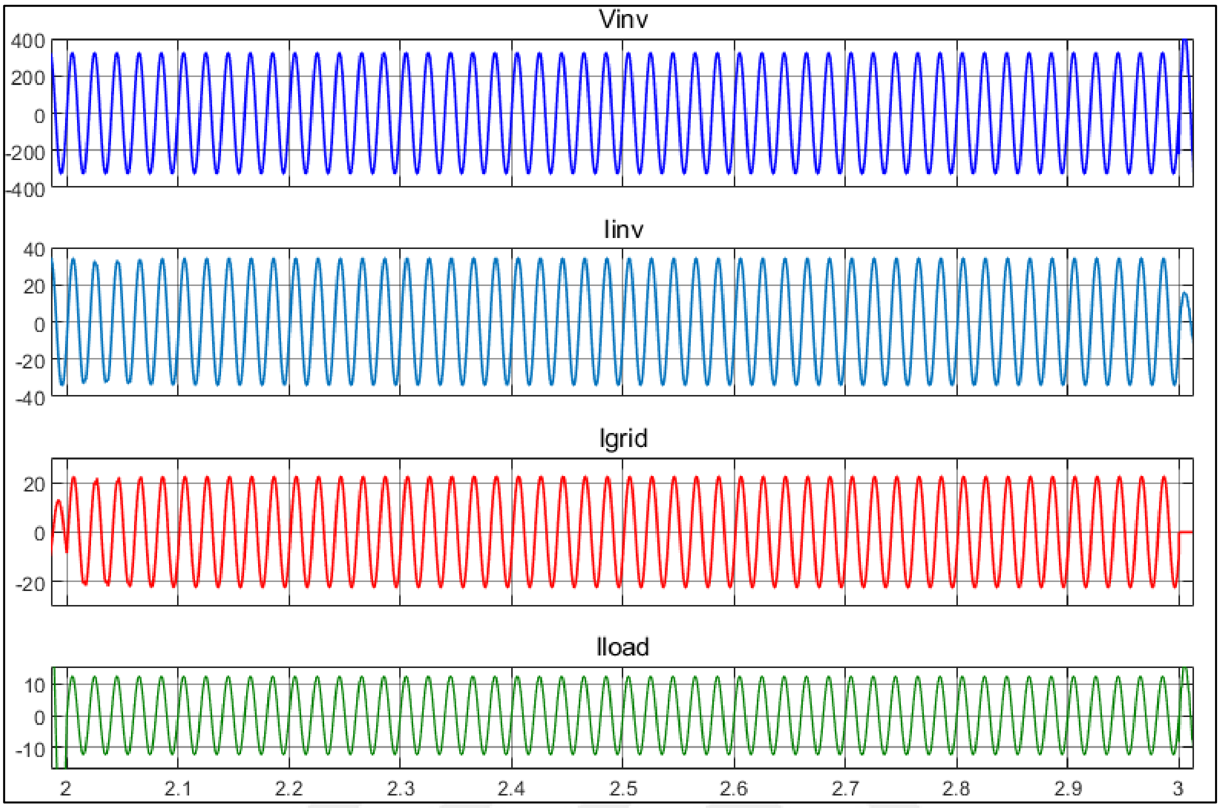

Figure 4.4. Case 1, Mode 1, from 2 to 3 seconds.

Finally, in Mode 3 from 3 to 4 seconds, the fuel cell operates at 2676 W, precisely matching the load demand of 2500 W. In this mode, there is no power exchange with the grid, as the generated power is entirely consumed by the load. This mode highlights the QZSI system's ability to balance power generation and consumption, maintaining stable operation without requiring grid interaction.

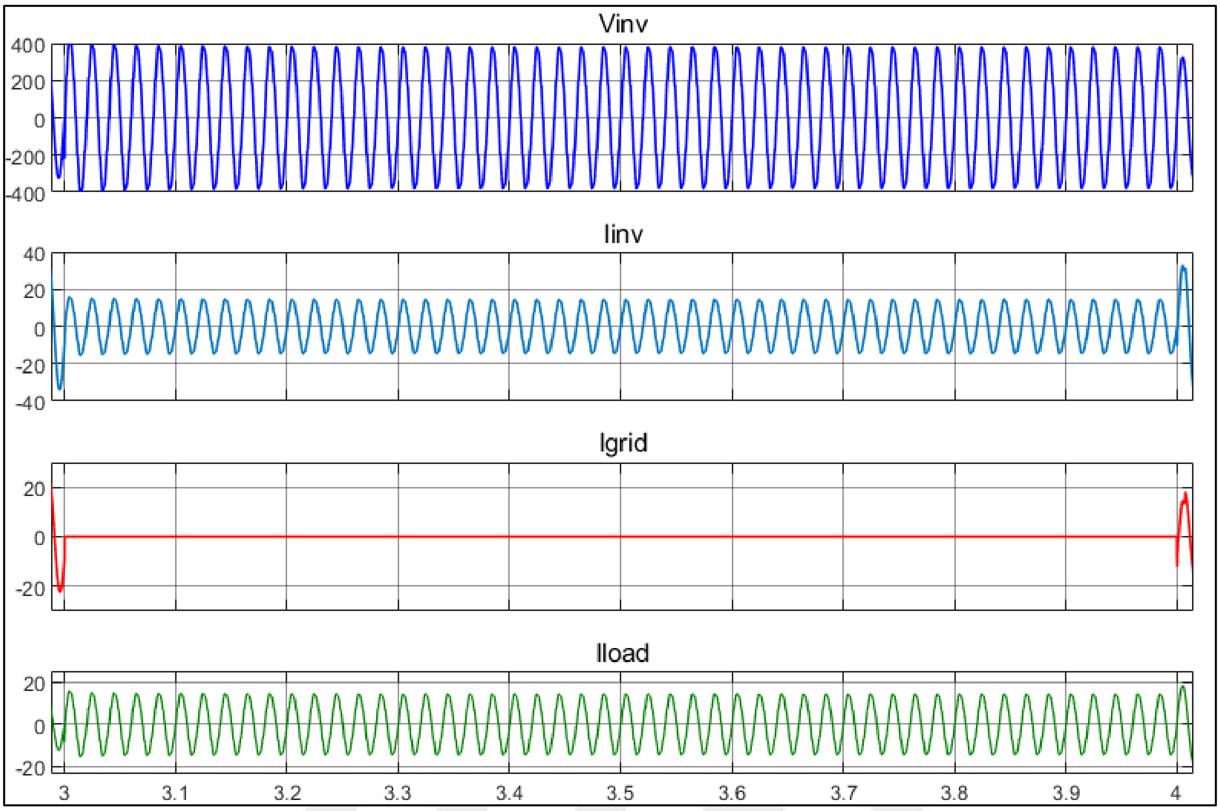

Figure 4.5. Case 1, Mode 3, from 3 to 4 seconds.

Overall, this detailed analysis of Case 1 showcases the QZSI system's flexibility and efficiency in managing power flows between the fuel cell, the load, and the grid under varying conditions. The system's ability to feed excess power into the grid, draw power to meet deficits, and balance generation and consumption without grid interaction demonstrates its robustness and reliability in dynamic power management scenarios.

These capabilities are essential for integrating renewable energy sources like fuel cells into modern power systems, ensuring efficient and stable energy supply. The results have been presented in Table 4.4.

Table 4.4. Case 1 Results.

	Simulation Time Interval	Fuel Cell Parameters	Fuel Cell Power	Load Power	Grid Power	Operation Mode	Efficiency
Case #1	t = 0-1 s	ST = 973 K FP = 1.35 bar	5730 W	P_{load} = 1000 W	- 4401 W	Mode 1	%94.26
	t = 1-2 s	ST = 973 K FP = 1.15 bar	5746 W	P_{load} = 7000 W	1593 W	Mode 2	%94.09
	t = 2-3 s	ST = 923 K FP = 1.0 bar	5819 W	P_{load} = 2000 W	-3403 W	Mode 1	%92.86
	t = 3-4 s	ST = 923 K FP = 1.0 bar	2676 W	P_{load} = 2500 W	0 W	Mode 3	%93.38

In Case 2, the QZSI system's performance is assessed over a four-second interval, covering different operational modes that illustrate the system's adaptability to varying load demands and fuel cell power outputs. This analysis underscores the system's efficiency in managing power flow between the fuel cell, the load, and the grid.

During Mode 1, from 4 to 5 seconds, the fuel cell operates at 5777 W, supplying a load of 3000 W. The excess power of 2608 W is fed into the grid, showcasing the system's capability to efficiently handle surplus power generation and support the grid. This mode highlights the QZSI's role in enhancing grid stability by contributing excess power generated by the fuel cell.

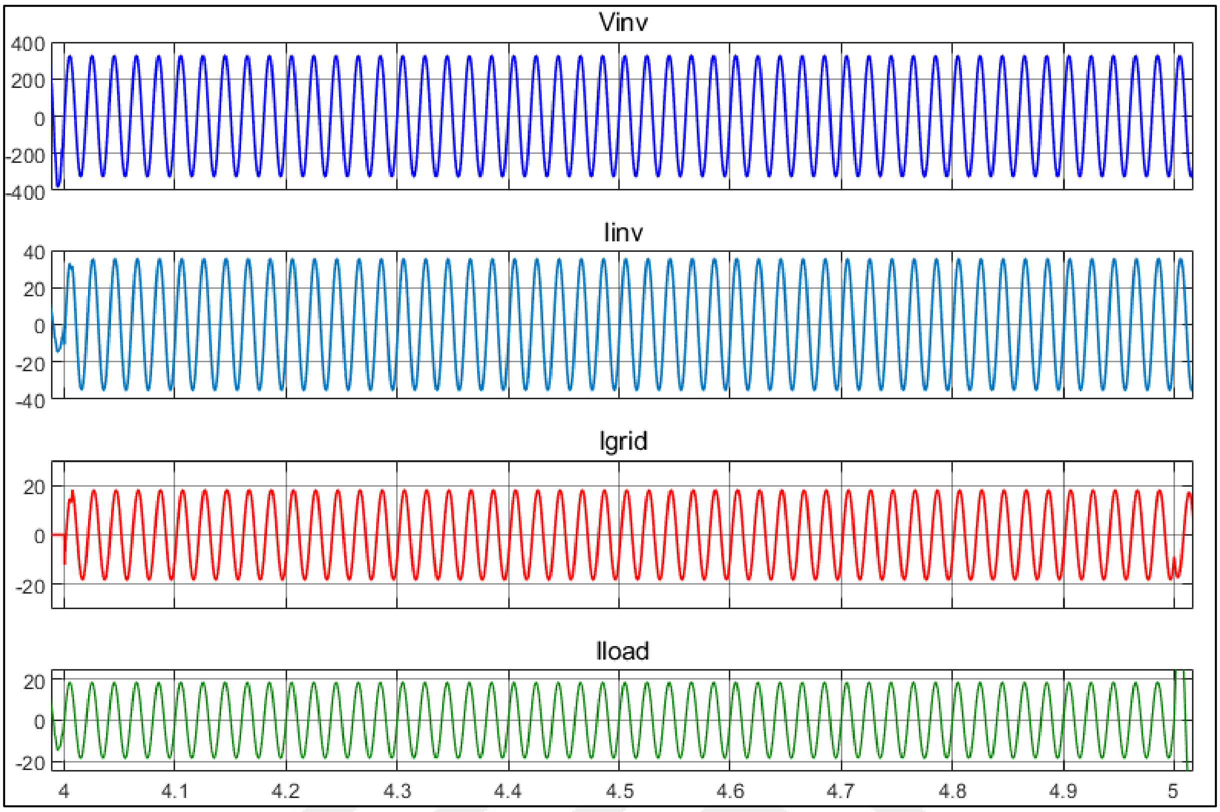

Figure 4.6. Case 2, Mode 1, from 4 to 5 seconds.

In Mode 2, from 5 to 6 seconds, the fuel cell maintains a power output of 5784 W, while the load demand increases significantly to 8000 W. This results in a power deficit of 2566 W, which is compensated by drawing additional power from the grid. This scenario demonstrates the QZSI system's flexibility in meeting high load demands by seamlessly integrating grid power, ensuring uninterrupted power supply to the load.

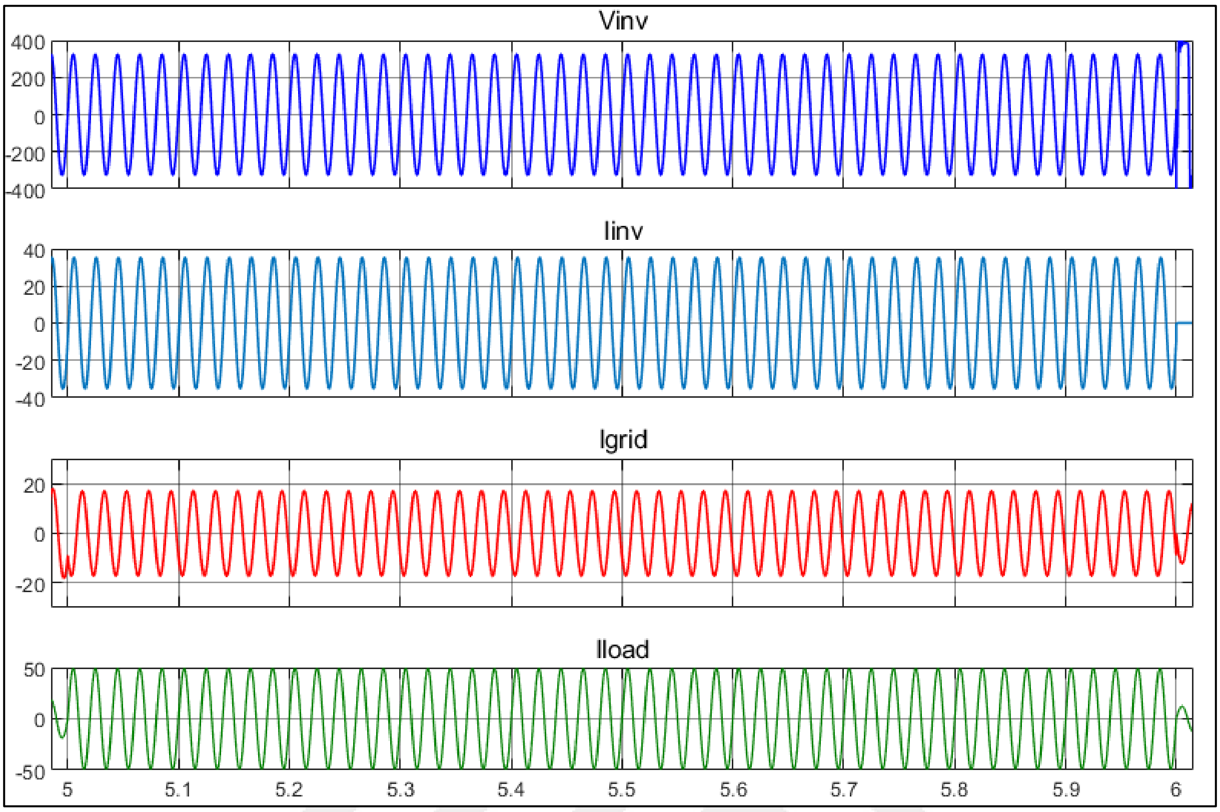

Figure 4.7. Case 2, Mode 2, from 5 to 6 seconds.

Mode 4, from 6 to 7 seconds, presents a scenario where the fuel cell is turned off, and the entire load of 2000 W is supplied solely by the grid. This mode illustrates the QZSI system's ability to rely on grid power when the fuel cell is not operational, maintaining continuous power delivery to the load without interruption. It underscores the importance of grid connectivity in providing a reliable backup power source.

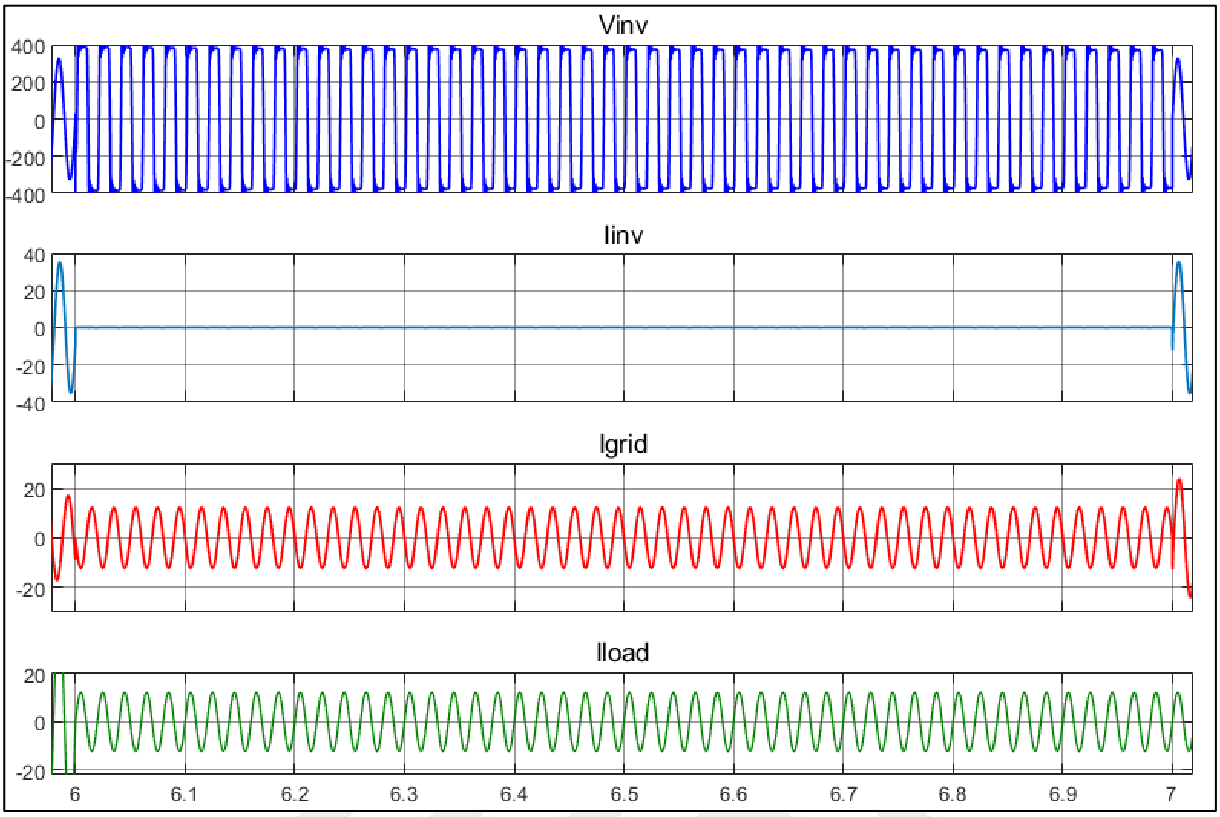

Figure 4.8. Case 2, Mode 4, from 6 to 7 seconds.

Returning to Mode 1 from 7 to 8 seconds, the fuel cell resumes operation at 5797 W, supplying a load of 2000 W. The excess power of 3444 W is again fed into the grid. This scenario reaffirms the system's efficiency in managing surplus power generation and supporting the grid by feeding back the excess power. The system's ability to dynamically adjust to changes in load demand and fuel cell operation is critical for maintaining optimal performance and grid stability.

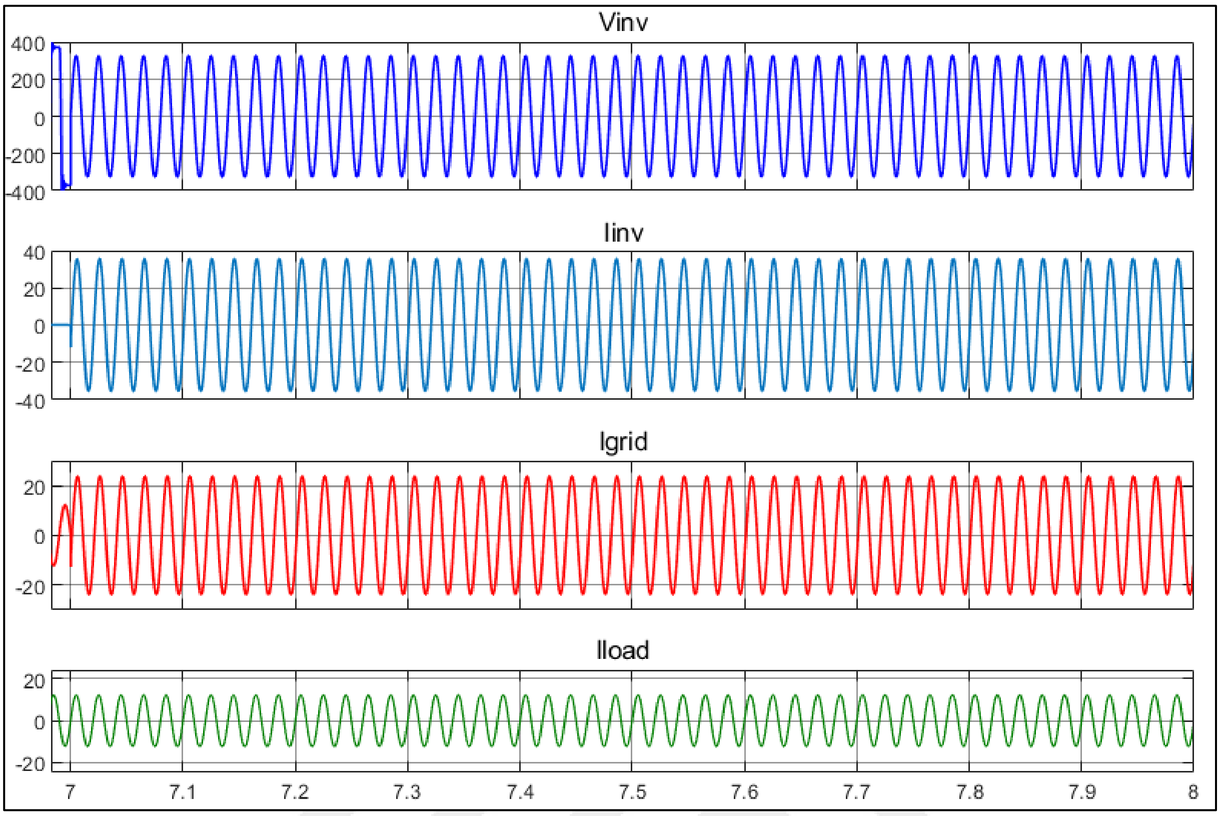

Figure 4.9. Case 2, Mode 1, from 7 to 8 seconds.

The analysis of Case 2 highlights the QZSI system's robustness and adaptability in various operational scenarios. The system effectively manages power flow by feeding excess power into the grid, drawing power to meet deficits, and relying on grid power when the fuel cell is off. These capabilities are essential for integrating renewable energy sources like fuel cells into modern power systems, ensuring efficient, reliable, and stable energy supply. The ability to seamlessly transition between different operational modes without compromising power quality or reliability demonstrates the QZSI system's suitability for dynamic and demanding energy environments. The results of this case study are presented in Table 4.5.

Table 4.5. Case 2 Results.

	Simulation Time Interval	Fuel Cell Parameters	Fuel Cell Power	Load Power	Grid Power	Operation Mode	Efficiency
Case #2	t = 4-5 s	ST = 973 K FP = 1.15 bar	6016 W	P_{load} = 3000 W	-2621 W	Mode 1	%93.44
	t = 5-6 s	ST = 973 K FP = 1.15 bar	6011 W	P_{load} = 8000 W	2382 W	Mode 2	%93.45
	t = 6-7 s	ST = 973 K FP = 0 bar	0 W	P_{load} = 2000 W	2000 W	Mode 4	N/A
	t = 7-8 s	ST = 973 K FP = 1.15 bar	6059 W	P_{load} = 2000 W	-3654 W	Mode 1	%93.33

These scenarios demonstrate the QZSI's ability to manage different load conditions and efficiently distribute power between the fuel cell and the grid.

The performance of the QZSI was evaluated by examining key parameters such as output voltage, current, THD, and efficiency under the varying load conditions described in Case 1 and Case 2.

The QZSI demonstrated high efficiency and stable output voltage in Mode 1, effectively managing surplus energy by feeding it back into the grid, thereby supporting grid stability and maximizing energy utilization. In Mode 2, the QZSI maintained stable output under increased load demand, showcasing its robustness in handling power deficits by drawing necessary power from the grid, ensuring high performance. Mode 3 highlighted the QZSI's capability to match load demand without grid interaction, making it suitable for standalone operations requiring grid independence and reliability. In Mode 4, the system showed flexibility by seamlessly switching to grid power when the fuel cell was off, ensuring uninterrupted power supply and enhancing overall system reliability.

Figure 4.10 presents a comparison between the Fuel Cell output voltage (Vin) and the DC link voltage of the inverter (V_{DC}) over the simulation period. The blue line represents the FC output voltage (Vin), while the orange line represents the DC link voltage of the inverter (V_{DC}).

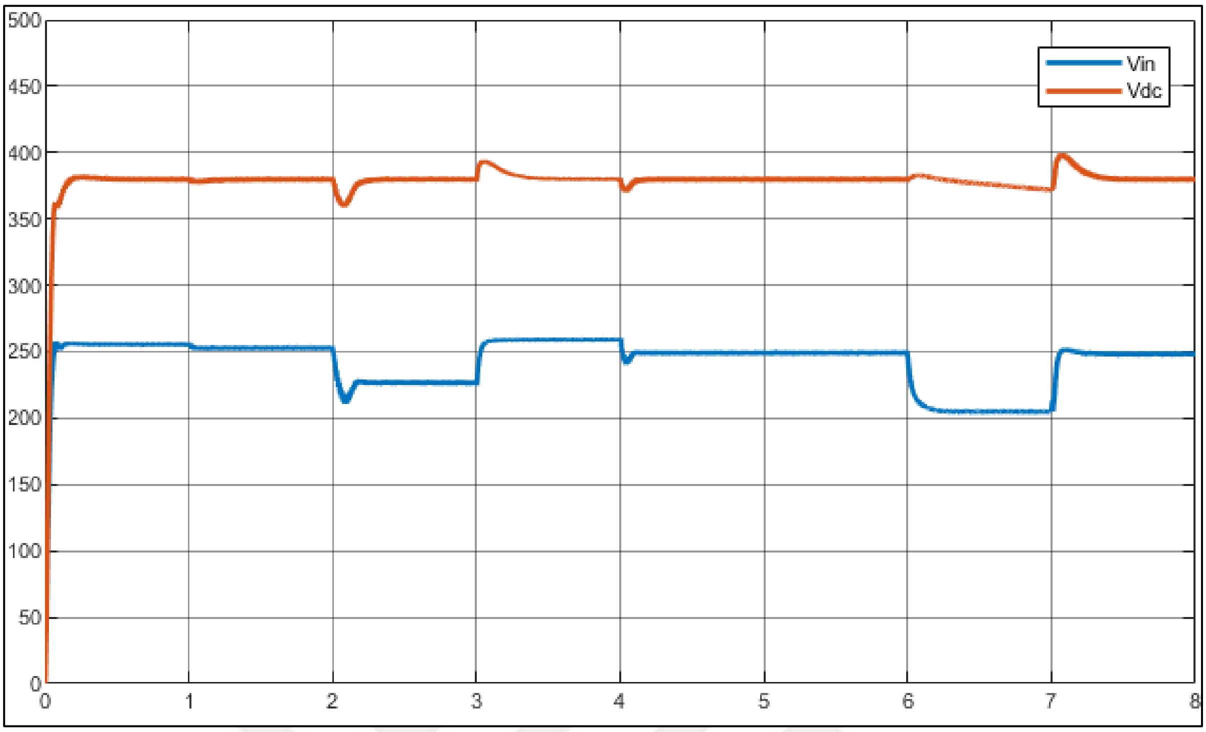

Figure 4.10. DC link voltage compared to the FC output voltage.

Initially, from 0 to 1 second, both *Vin* and V_{DC} exhibit a sharp rise as they stabilize at their respective operating levels. The FC output voltage (*V*in) quickly settles around 250V, while the DC link voltage (V_{DC}) stabilizes at a higher level, around 380V. This initial phase indicates the system's ability to rapidly achieve steady-state operation after startup.

Around the 2-second mark, a transient response is observed, characterized by small dips in both *Vin* and V_{DC}. *Vin* drops slightly below 250V, suggesting a brief disturbance, possibly due to a change in load or an adjustment in the control system. Correspondingly, V_{DC} shows a minor dip but maintains its relative level above *Vin*, albeit slightly lower than its initial steady-state value. This behavior highlights the system's sensitivity to transient changes and its capacity to quickly stabilize.

Between 2 and 6 seconds, the voltages demonstrate intermediate stability with minor fluctuations. *Vin* fluctuates slightly around 250V, and another minor dip occurs around the 3-second mark. Despite these variations, V_{DC} continues to remain stable around 380V, indicating effective voltage regulation by the inverter system. A significant dip is observed around the 6-

second mark, where *Vin* decreases to approximately 200V, and V_{DC} shows a corresponding drop. This dip suggests a more substantial disturbance or a control action that temporarily affects the voltages.

Following the significant dip at 6 seconds, both voltages recover and stabilize again from 6 to 8 seconds. V_{in} returns to its steady-state value around 250V, and V_{DC} also returns to its previous steady-state value around 380V, maintaining its higher relative voltage above *Vin*. This recovery phase underscores the system's capability to handle significant disturbances and return to stable operation.

Throughout the entire period, the DC link voltage (V_{DC}) consistently remains higher than the FC output voltage (V_{in}), demonstrating the effective voltage boosting capability of the Quasi-Z Source stage of the inverter system. The observed transient dips and subsequent quick recoveries highlight the robustness of the control system in stabilizing the voltages and ensuring consistent performance despite transient disturbances.

The interaction between the QZSI, the fuel cell, and the grid was analyzed to understand the system's overall dynamics. The fuel cell provided a stable DC voltage, which the QZSI converted to AC power for grid connection. The inverter's shoot-through capability allowed for effective voltage boosting, ensuring consistent power supply to the grid despite fluctuations in the fuel cell's output. The comparison of inverter output voltage and current with grid and load currents during both case studies is depicted in Figure 4.11.

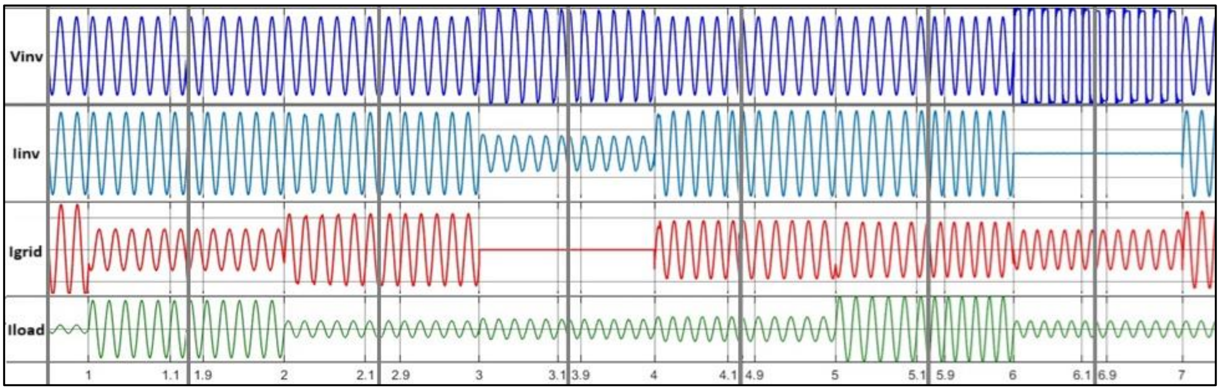

Figure 4.11. Signal form and phase changes during transitions.

The phase changes between the inverter output, grid, and load currents are an indication for effective power flow and synchronization. The inverter output voltage and current are in phase, ensuring efficient active power conversion from DC to AC. The initial transients in the grid current suggest phase adjustments during transition from the previous working mode. Once stabilized, the grid current aligns with the inverter output, ensuring seamless power transfer to the grid. The load current variations reflect dynamic load conditions, but the overall sinusoidal shape indicates stable power delivery.

Overall, the waveforms demonstrate the inverter's ability to produce stable output, synchronize with the grid, and supply the load with consistent power, highlighting its reliability and efficiency in a grid-connected setup. The complete results of Case 1 and Case 2 are shown in Figure 4.12 and Figure 4.13.

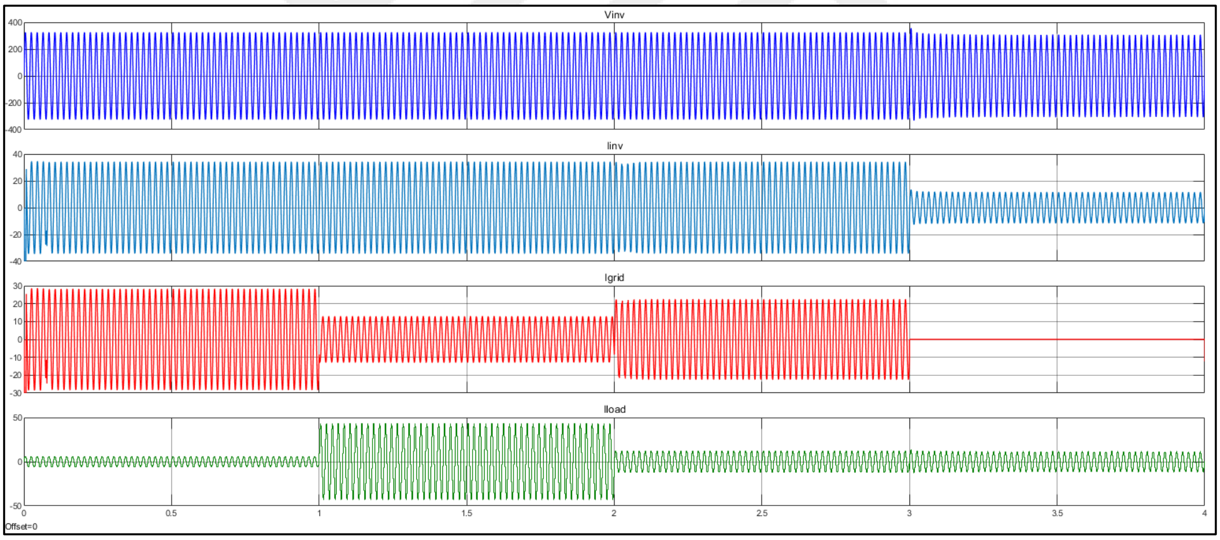

Figure 4.12. Overall Case 1 Results.

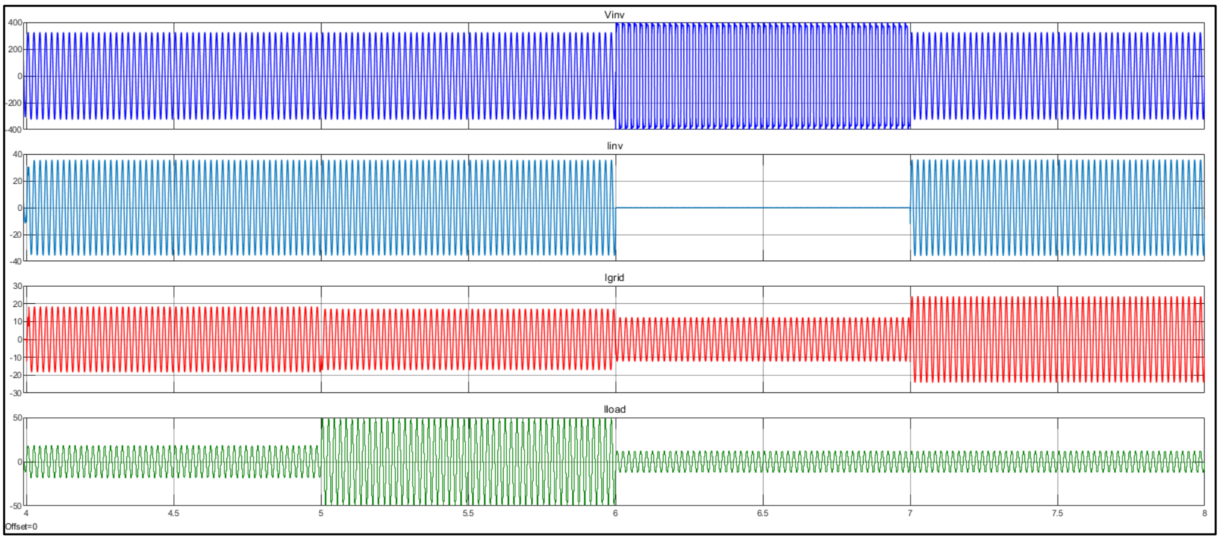

Figure 4.13. Overall Case 2 Results.

The comparison of fuel cell power and inverter power along with the overall system efficiency has been presented in Figure 4.14.

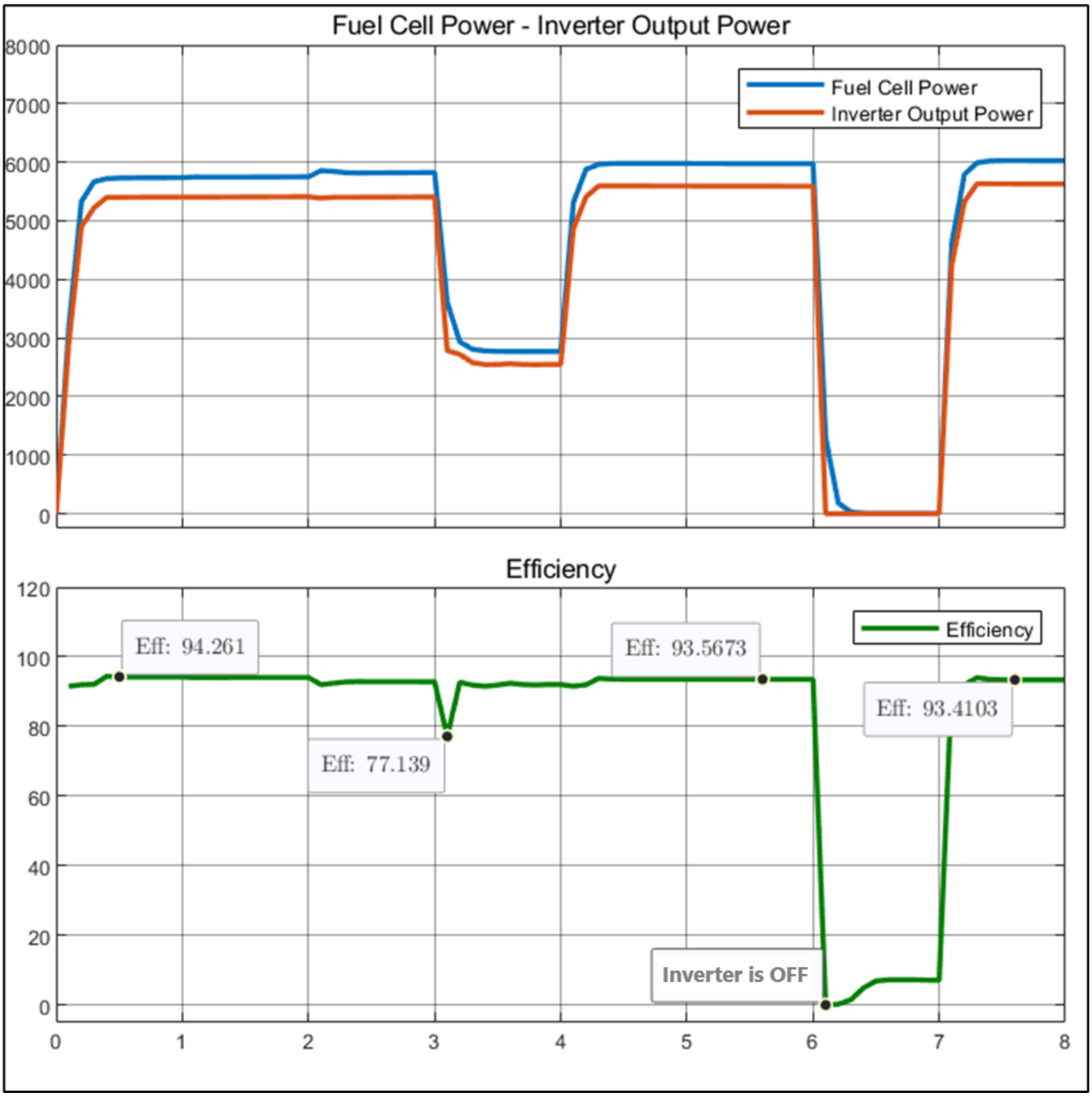

Figure 4.14. Comparison of fuel cell and inverter output powers.

The graph illustrates the relationship between the fuel cell power, which supplies the inverter, and the inverter's output power, along with the system's efficiency under different operating conditions. Initially, the fuel cell delivers around 5500 W, with the inverter outputting slightly less due to conversion losses. At approximately 2 seconds, a sharp reduction in both fuel cell and inverter power is observed, reflecting the dynamic behavior of the system in response to load changes. After this event, the system stabilizes, with power levels recovering.

The system's efficiency, as shown in the lower plot, begins at a peak of 94.26% before experiencing a minor decrease. The sharp power reduction is accompanied by a drop in efficiency to 77.14%, followed by recovery to over 93%. Overall, the system demonstrates strong performance, with transient conditions briefly affecting efficiency.

The comparison of THD before and after the LCL filter stage in Figure 4.15.

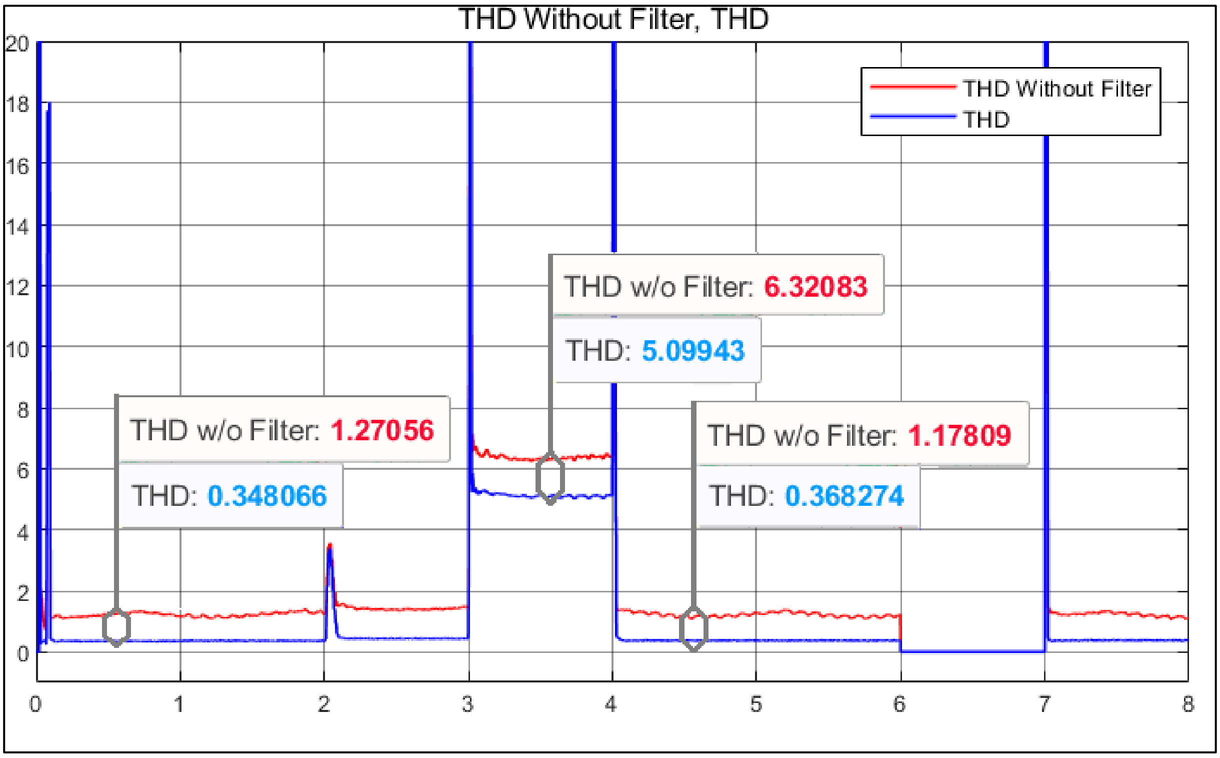

Figure 4.15 THD results with and without the LCL filter.

The graph displays the Total Harmonic Distortion (THD) with and without the filter applied, where the red line represents the unfiltered THD and the blue line shows the filtered THD. Initially, the THD reaches around 18%, then shortly, the THD is reduced significantly by the filter and the modulation to below 1%. Throughout the simulation, high peaks in the THD occur due to dynamic system behavior and load changes, particularly between 3 and 4 seconds, where the grid is disconnected and the reference voltage is affected. Despite these peaks, the filter remains effective, keeping the THD low.

At the 6-second mark, the THD drops to zero due to the inverter being disconnected from the system. Throughout the simulation, the average unfiltered THD remains below 2%, while the filtered THD maintains an average of approximately 0.35%. This demonstrates the filter’s effectiveness in significantly reducing harmonic distortion under various operating conditions, maintaining overall system performance.

4.3. Comparison with Theoretical Expectations and Previous Studies

The simulation results were compared with theoretical expectations and findings from previous studies to validate the QZSI's performance:

- The QZSI's ability to maintain high efficiency and low THD under various load conditions was consistent with theoretical predictions and previous research [68].
- The dynamic performance under variable load scenarios aligned well with earlier studies, highlighting the inverter's robustness and reliability [69].
- The interaction between the QZSI, fuel cell, and grid showed improved system stability and efficiency, supporting findings from other researchers who have explored similar setups [70].

4.4. Discussion

The primary objective of this research was to evaluate the performance of the QZSI integrated with a fuel cell as the primary DC source under various load conditions. The simulation results demonstrated that the QZSI effectively managed different load scenarios specified in Case 1 and Case 2. The inverter maintained high efficiency, low THD, and stable output voltage across all tested conditions. These findings confirm that the QZSI is suitable for applications involving renewable energy sources, providing reliable performance even with fluctuating inputs and varying loads.

Several key findings emerged from the study:

1. **High Efficiency and Low THD:** The QZSI maintained high efficiency and low THD under various load conditions, demonstrating its capability to deliver clean and stable power. This is crucial for grid-tied applications where power quality is paramount.

2. **Robust Performance Under Variable Loads:** The inverter handled both steady and dynamic loads effectively, ensuring consistent output and efficient power management. This robustness is beneficial for real-world applications where load demands can vary significantly.
3. **Effective Integration with Fuel Cells:** The QZSI demonstrated reliable performance with the fuel cell as the primary DC source, efficiently managing the power flow between the fuel cell and the grid. This indicates the potential of QZSIs in renewable energy systems, especially those utilizing fuel cells.
4. **AC-to-DC conversion:** These findings imply that QZSIs can significantly enhance the efficiency and reliability of renewable energy systems, making them a viable option for both residential and commercial applications.

While the study provided valuable insights into the performance of QZSIs, there were several limitations:

1. **Simulation-Based Analysis:** The study was conducted using simulations, which, while useful, may not capture all real-world complexities. Experimental validation is necessary to confirm the simulation results and will be defined as future work.
2. **Limited Load Scenarios:** Only specific load scenarios were tested. Future research should explore a broader range of conditions, including more complex and varied load profiles, to comprehensively evaluate the inverter's performance. This will be defined as a future work to achieve on the experimental setup.

5. CONCLUSION

5.1.1. Summary of the Main Findings

This research focused on evaluating the performance of the QZSI integrated with a fuel cell under various load conditions using MATLAB/Simulink simulations. The main findings of this study are as follows:

1. **High Efficiency and Low THD:** The QZSI maintained high efficiency and low THD across all tested load conditions, demonstrating its capability to deliver clean and stable power, which is crucial for grid-tied applications.
2. **Robust Performance Under Variable Loads:** The inverter effectively managed both steady and dynamic loads, ensuring consistent output and efficient power management. This robustness is beneficial for real-world applications in which load demands can vary significantly.
3. **Effective Integration with Fuel Cells:** The QZSI demonstrated reliable performance with the fuel cell as the primary DC source, efficiently managing the power flow between the fuel cell and grid. This indicates the potential of QZSIs in renewable energy systems, especially those utilizing fuel cells.

5.1.2. Contribution of the Research to the Field

This research contributes to the field of power electronics and renewable energy systems by providing a comprehensive analysis of the performance of QZSIs when integrated with fuel cells. The key contributions of this study include the following:

1. **Validation of QZSI Efficiency and Stability:** This study validated the high efficiency and stability of QZSIs under various load conditions, supporting their use in grid-tied and standalone renewable energy applications.
2. **Integration with Renewable Energy Sources:** The study highlights the effective integration of QZSIs with fuel cells, providing a viable solution for renewable energy systems that require efficient and reliable power conversion technologies.

6. RECOMMENDATIONS

While this study has provided significant insights into the performance of QZSIs, further research is recommended in the following areas:

1. **Experimental Validation:** Future work should include real-world experiments to validate the simulation results and address any discrepancies between the theoretical and practical outcomes.
2. **Extended Load Testing:** Additional studies should explore a wider variety of load conditions, including non-linear and unbalanced loads, to comprehensively evaluate the performance of the inverter.
3. **Advanced Control Techniques:** Further optimization of control strategies, including the exploration of advanced algorithms, could enhance the efficiency, stability, and response time of QZSIs.
4. **Integration with Multiple Renewable Sources:** Investigating the performance of QZSIs when integrated with other renewable energy sources such as solar or wind, in addition to fuel cells, would provide a broader understanding of their versatility and applicability.
5. **Addressing Limitations:** Research should focus on addressing the identified limitations, such as the need for larger inductance and capacitance in single-phase QZSIs to limit switching frequency ripple, and finding solutions to reduce component stresses.

By addressing these areas, future research can further solidify the role of QZSIs in enhancing the efficiency and reliability of renewable energy systems, paving the way for their broader adoption in various applications.

REFERENCES

[1] Y. Liu, H. Abu-Rub, and B. Ge, “Z-source/quasi-Z-source inverters: Derived networks, modulations, controls, and emerging applications to photovoltaic conversion,” *IEEE Industrial Electronics Magazine*, vol. 8, no. 4, pp. 32–44, 2014, doi: 10.1109/MIE.2014.2307898.

[2] A. A. Khan, H. Cha, H. F. Ahmed, J. Kim, and J. Cho, “A Highly Reliable and High-Efficiency Quasi Single-Stage Buck-Boost Inverter,” *IEEE Trans Power Electron*, vol. 32, no. 6, pp. 4185–4198, Jun. 2017, doi: 10.1109/TPEL.2016.2598251.

[3] Y. Liu, B. Ge, H. Abu-Rub, and F. Z. Peng, “An effective control method for quasi-Z-source cascade multilevel inverter-based grid-tie single-phase photovoltaic power system,” *IEEE Transactions on Industrial Informatics*, vol. 10, no. 1, pp. 399–407, Feb. 2014, doi: 10.1109/TII.2013.2280083.

[4] F. Blaabjerg, Z. Chen, and S. B. Kjaer, “Power electronics as efficient interface in dispersed power generation systems,” *IEEE Trans Power Electron*, vol. 19, no. 5, pp. 1184–1194, Sep. 2004, doi: 10.1109/TPEL.2004.833453.

[5] J. Rodríguez, J. S. Lai, and F. Z. Peng, “Multilevel inverters: A survey of topologies, controls, and applications,” *IEEE Transactions on Industrial Electronics*, vol. 49, no. 4, pp. 724–738, Aug. 2002, doi: 10.1109/TIE.2002.801052.

[6] P. R. Bana, K. P. Panda, R. T. Naayagi, P. Siano, and G. Panda, “Recently Developed Reduced Switch Multilevel Inverter for Renewable Energy Integration and Drives Application: Topologies, Comprehensive Analysis and Comparative Evaluation,” *IEEE Access*, vol. 7, pp. 54888–54909, 2019, doi: 10.1109/ACCESS.2019.2913447.

[7] J. S. Lai and F. Z. Peng, “Multilevel converters - a new breed of power converters,” *Conference Record - IAS Annual Meeting (IEEE Industry Applications Society)*, vol. 3, pp. 2348–2356, 1995, doi: 10.1109/IAS.1995.530601.

[8] D. G. Holmes and T. A. Lipo, *Width Modulation for Power Converters*, 2003.

[9] Y. Li, J. Anderson, F. Z. Peng, and L. Dichen, “Quasi-z-source inverter for photovoltaic power generation systems,” *Conference Proceedings - IEEE Applied Power Electronics Conference and Exposition - APEC*, pp. 918–924, 2009, doi: 10.1109/APEC.2009.4802772.

[10] A. Liske, G. Clos, and M. Braun, "Analysis and modeling of the Quasi-Z-Source-Inverter," *IECON Proceedings (Industrial Electronics Conference)*, pp. 1197–1202, 2011, doi: 10.1109/IECON.2011.6119479.

[11] I. S. Fedin, T. O. Tereshchenko, and Y. S. Yamnenko, "Quasi-Z-Source Inverters in Renewable Power Systems Modeling," *Microsystems, Electronics and Acoustics*, vol. 26, no. 3, pp. 237407-1-237407–7, Dec. 2021, doi: 10.20535/2523-4455.MEA.237407.

[12] H. Bai, F. Wang, X. Yu, and G. Lin, "An Improved Model Predictive Control Algorithm for Quasi-Z-Source Inverter," *Proceedings of 2019 IEEE 3rd Advanced Information Management, Communicates, Electronic and Automation Control Conference, IMCEC 2019*, pp. 385–390, Oct. 2019, doi: 10.1109/IMCEC46724.2019.8984138.

[13] J. Larminie and A. Dicks, *Fuel Cell Systems Explained: Second Edition*, pp. 1–406, Dec. 2013, doi: 10.1002/9781118878330.

[14] A. J. . Appleby and F. R. . Foulkes, *Fuel cell handbook*, p. 762, 1993.

[15] S. P. Jiang and Q. Li, "Phosphoric Acid Fuel Cells," *Introduction to Fuel Cells*, pp. 649–671, 2022, doi: 10.1007/978-981-10-7626-8_14.

[16] S. C. Singhal, "Solid oxide fuel cells for power generation," *Wiley Interdiscip Rev Energy Environ*, vol. 3, no. 2, pp. 179–194, Mar. 2014, doi: 10.1002/WENE.96.

[17] T. Leo, "Molten Carbonate Fuel Cells: Theory and Application," *Comprehensive Renewable Energy*, pp. 247–259, Jan. 2012, doi: 10.1016/B978-0-08-087872-0.00408-X.

[18] H. Kim and S. K. Sul, "Analysis on output LC filters for PWM inverters," *2009 IEEE 6th International Power Electronics and Motion Control Conference, IPEMC '09*, pp. 384–389, 2009, doi: 10.1109/IPEMC.2009.5157417.

[19] S. Jayalath and M. Hanif, "Generalized LCL-Filter Design Algorithm for Grid-Connected Voltage-Source Inverter," *IEEE Transactions on Industrial Electronics*, vol. 64, no. 3, pp. 1905–1915, Mar. 2017, doi: 10.1109/TIE.2016.2619660.

[20] S. Pöhler, A. Mertens, and R. Sommer, "Optimisation of output filters for inverter fed drives," *IECON Proceedings (Industrial Electronics Conference)*, pp. 1082–1088, 2006, doi: 10.1109/IECON.2006.347319.

[21] Y. Sozer, D. A. Torrey, and S. Reva, "New inverter output filter topology for PWM motor drives," *IEEE Trans Power Electron*, vol. 15, no. 6, pp. 1007–1017, Nov. 2000, doi: 10.1109/63.892815.

[22] M. F. Arman, C. C. Marouchos, and M. K. Darwish, "Self-tuning output passive-filter for low power DC/AC inverters," *Proceedings of the Universities Power Engineering Conference*, 2012, doi: 10.1109/UPEC.2012.6398596.

[23] E. Samadaei, S. A. Gholamian, A. Sheikholeslami, and J. Adabi, "An Envelope Type (E-Type) Module: Asymmetric Multilevel Inverters with Reduced Components," *IEEE Transactions on Industrial Electronics*, vol. 63, no. 11, pp. 7148–7156, Nov. 2016, doi: 10.1109/TIE.2016.2520913.

[24] W. Liang, B. Ge, Y. Liu, H. Abu-Rub, R. S. Balog, and Y. Xue, "Modeling, analysis, and impedance design of battery energy stored single-phase quasi-Z source photovoltaic inverter system," *ECCE 2016 - IEEE Energy Conversion Congress and Exposition, Proceedings*, 2016, doi: 10.1109/ECCE.2016.7855265.

[25] Y. Zhou, H. Li, and H. Li, "A single-phase PV quasi-Z-source inverter with reduced capacitance using modified modulation and double-frequency ripple suppression," *IEEE Trans Power Electron*, vol. 31, no. 3, pp. 2166–2173, Mar. 2016, doi: 10.1109/TPEL.2015.2432070.

[26] Y. Liu, B. Ge, H. Abu-Rub, and H. Sun, "Hybrid Pulsewidth Modulated Single-Phase Quasi-Z-Source Grid-Tie Photovoltaic Power System," *IEEE Transactions on Industrial Informatics*, vol. 12, no. 2, pp. 621–632, Apr. 2016, doi: 10.1109/TII.2016.2524561.

[27] A. R. Suryawanshi and N. B. Chopade, "Multilevel Inverter Topologies and Modulation Techniques for Grid Connection of Renewable Energy Source," *Proceeding - 1st International Conference on Innovative Trends and Advances in Engineering and Technology, ICITAET 2019*, pp. 227–232, Dec. 2019, doi: 10.1109/ICITAET47105.2019.9170239.

[28] F. Z. Peng, W. Qian, and D. Cao, "Recent advances in multilevel converter/inverter topologies and applications," *2010 International Power Electronics Conference - ECCE Asia -, IPEC 2010*, pp. 492–501, 2010, doi: 10.1109/IPEC.2010.5544625.

[29] J. A. F. Neto, R. P. T. Bascope, C. M. Cruz, R. G. A. Cacau, and G. V. T. Bascope, "Comparative evaluation of three single-phase NPC inverters," *2012 10th IEEE/IAS International Conference on Industry Applications, INDUSCON 2012*, 2012, doi: 10.1109/INDUSCON.2012.6453691.

[30] M. İnci, "Performance Evaluation of Multi-carrier PWM Techniques: PD, POD and APOD," *International Journal of Applied Mathematics Electronics and Computers*, vol. 7, no. 2, pp. 38–43, Jun. 2019, doi: 10.18100/IJAMEC.569660.

[31] A. Bakeer, I. S. Mohamed, P. B. Malidarreh, I. Hattabi, and L. Liu, "An Artificial Neural Network-Based Model Predictive Control for Three-Phase Flying Capacitor Multilevel Inverter," *IEEE Access*, vol. 10, pp. 70305–70316, 2022, doi: 10.1109/ACCESS.2022.3187996.

[32] E. Parimalasundar, R. Jayanthi, K. Suresh, and R. Sindhuja, "Investigation of efficient multilevel inverter for photovoltaic energy system and electric vehicle applications," *Electrical Engineering & Electromechanics*, vol. 2023, no. 4, pp. 47–51, Jun. 2023, doi: 10.20998/2074-272X.2023.4.07.

[33] Y. Yu, G. Konstantinou, B. Hredzak, and V. G. Agelidis, "Power Balance Optimization of Cascaded H-Bridge Multilevel Converters for Large-Scale Photovoltaic Integration," *IEEE Trans Power Electron*, vol. 31, no. 2, pp. 1108–1120, Feb. 2016, doi: 10.1109/TPEL.2015.2407884.

[34] Y. Li, S. Jiang, J. G. Cintron-Rivera, and F. Z. Peng, "Modeling and control of quasi-z-source inverter for distributed generation applications," *IEEE Transactions on Industrial Electronics*, vol. 60, no. 4, pp. 1532–1541, 2013, doi: 10.1109/TIE.2012.2213551.

[35] U. K. Shinde, S. G. Kadwane, S. P. Gawande, M. J. B. Reddy, and D. K. Mohanta, "Sliding Mode Control of Single-Phase Grid-Connected Quasi-Z-Source Inverter," *IEEE Access*, vol. 5, pp. 10232–10240, 2017, doi: 10.1109/ACCESS.2017.2708720.

[36] H. Abu-Rub, A. Iqbal, S. M. Ahmed, F. Z. Peng, Y. Li, and G. Baoming, "Quasi-Z-source inverter-based photovoltaic generation system with maximum power tracking control using ANFIS," *IEEE Transactions on Sustainable Energy*, vol. 4, no. 1, pp. 11–20, 2013, doi: 10.1109/TSTE.2012.2196059.

[37] H. Zhang, B. Ge, Y. Liu, H. Abu-Rub, D. Sun, and F. Z. Peng, "A hybrid modulation method for single-phase quasi-Z source inverter," *2014 IEEE Energy Conversion Congress and Exposition, ECCE 2014*, pp. 4444–4449, Nov. 2014, doi: 10.1109/ECCE.2014.6953729.

[38] Y. Rekha, I. W. Christopher, and V. Jamuna, "Fuel Cell Based Sl Quasi Z-Source Inverter for Motor Drive," *5th International Conference on Electrical Energy Systems, ICEES 2019*, May 2019, doi: 10.1109/ICEES.2019.8719296.

[39] M. Meraj, A. Iqbal, L. Brahim, R. Alammari and H. Abu-Rub, "A high efficiency and high reliability single-phase modified quasi Z-Source inverter for non-isolated grid-connected applications," IECON 2015 - 41st Annual Conference of the IEEE Industrial Electronics Society, Yokohama, Japan, 2015, pp. 004305-004310, doi: 10.1109/IECON.2015.7392770.

[40] M. Meraj, S. Rahman, A. Iqbal, and L. Ben-Brahim, "Common Mode Voltage Reduction in a Single-Phase Quasi Z-Source Inverter for Transformerless Grid-Connected Solar PV Applications," *IEEE Journal of Emerging and Selected Topics in Power Electronics*, vol. 7, no. 2, pp. 1352–1363, Jun. 2019, doi: 10.1109/JESTPE.2018.2867521.

[41] W. Miao, L. Ziguang, H. Likun, D. Aihua, and Z. Fei, "Quasi-Z-source inverter in grid-connected photovoltaic system," in *Proceedings of the 32nd Chinese Control Conference*, 2013, pp. 7595–7599.

[42] S. G. Patil and Rajashekar. J. S, "Simulation of Space Vector Modulated Quasi-Z-Source Cascade Multilevel Inverter for Grid-Tie based Single Phase PV System," *International Journal of Engineering Research & Technology*, vol. 3, no. 19, Apr. 2018, doi: 10.17577/IJERTCONV3IS19226.

[43] Y. Rekha, I. William Christopher, and V. Jamuna, "Quasi-ZSI topology for renewable energy system: A review," *International Conference on Power and Embedded Drive Control, ICPEDC 2017*, pp. 333–337, Oct. 2017, doi: 10.1109/ICPEDC.2017.8081110.

[44] S. S. Baligar, C. S. Kukanur, and C. K. Jambotkar, "Feasibility Study of Modified Quasi Z Source Inverter for Solar PV Technology," *International Journal of Trend in Scientific Research and Development*, vol. Volume-2, no. Issue-6, pp. 1327–1331, Oct. 2018, doi: 10.31142/IJTSRD18839.

[45] E. Babu, "Renewable Energy Sources Using Quasi-Z-Source Inverter With Distribution Level Power-Quality Improvement," *International Journal of Research and Engineering*, Mar. 2015, Accessed: Aug. 18, 2024. [Online]. Available: https://www.academia.edu/122516341/Renewable_Energy_Sources_Using_Quasi_Z_Source_Inverter_With_Distribution_Level_Power_Quality_Improvement

[46] A. Ayad, P. Karamanakos, and R. Kennel, "Direct model predictive current control strategy of quasi-Z-source inverters," *IEEE Trans Power Electron*, vol. 32, no. 7, pp. 5786–5801, Jul. 2017, doi: 10.1109/TPEL.2016.2610459.

[47] D. Cao, S. Jiang, X. Yu, and F. Z. Peng, "Low-cost semi-Z-source inverter for single-phase photovoltaic systems," *IEEE Trans Power Electron*, vol. 26, no. 12, pp. 3514–3523, 2011, doi: 10.1109/TPEL.2011.2148728.

[48] L. Zhang, K. Sun, L. Feng, H. Wu, and Y. Xing, "A family of neutral point clamped full-bridge topologies for transformerless photovoltaic grid-tied inverters," *IEEE Trans Power Electron*, vol. 28, no. 2, pp. 730–739, 2013, doi: 10.1109/TPEL.2012.2205406.

[49] W. Y. Choi and M. K. Yang, "Transformerless Quasi-Z-Source Inverter to Reduce Leakage Current for Single-Phase Grid-Tied Applications," *Electronics 2019, Vol. 8, Page 312*, vol. 8, no. 3, p. 312, Mar. 2019, doi: 10.3390/ELECTRONICS8030312.

[50] O. Husev, S. Stepenko, C. Roncero-Clemente, D. Vinnikov, and E. Romero-Cadaval, "Output filter design for grid connected single phase three-level quasi-Z-source inverter," *International Conference-Workshop Compatibility in Power Electronics , CPE*, pp. 46–51, 2013, doi: 10.1109/CPE.2013.6601127.

[51] B. Ge *et al.*, "Current ripple damping control to minimize impedance network for single-phase Quasi-Z source inverter system," *IEEE Transactions on Industrial Informatics*, vol. 12, no. 3, pp. 1043–1054, Jun. 2016, doi: 10.1109/TII.2016.2544246.

[52] L. Monjo, L. Sainz, J. J. Mesas, and J. Pedra, "Quasi-Z-Source Inverter-Based Photovoltaic Power System Modeling for Grid Stability Studies," *Energies 2021, Vol. 14, Page 508*, vol. 14, no. 2, p. 508, Jan. 2021, doi: 10.3390/EN14020508.

[53] X. Zhu, B. Zhang, and D. Qiu, "A High Boost Active Switched Quasi-Z-Source Inverter With Low Input Current Ripple," *IEEE Transactions on Industrial Informatics*, vol. 15, no. 9, pp. 5341–5354, Feb. 2019, doi: 10.1109/TII.2019.2899937.

[54] D. Vinnikov, I. Roasto, R. Strzelecki, and M. Adamowicz, "Step-up DC/DC converters with cascaded quasi-Z-source network," *IEEE Transactions on Industrial Electronics*, vol. 59, no. 10, pp. 3727–3736, 2012, doi: 10.1109/TIE.2011.2178211.

[55] A. Paikray, S. Prudhvi, and S. K. Nayak, "Improved Enhanced-Boost Quasi-Z-Source Inverter," *10th IEEE International Conference on Power Electronics, Drives and Energy Systems, PEDES 2022*, 2022, doi: 10.1109/PEDES56012.2022.10080512.

[56] M. Basic, D. Vukadinovic, and M. Polic, "Dynamic simulation model of a quasi-Z-Source inverter with parasitic resistances and saturable inductor," *19th International Symposium on Power Electronics, Ee 2017*, vol. 2017-December, pp. 1–6, Dec. 2017, doi: 10.1109/PEE.2017.8171663.

[57] S.-G. Lim and J. Choi, "LCL filter Design for Grid Connected NPC Type Three-Level Inverter," *International Journal of Renewable Energy Research*, 2015, doi: 10.20508/IJRER.50149.

[58] M. Dursun and M. K. Dosoglu, "LCL Filter Design for Grid Connected Three-Phase Inverter," *ISMSIT 2018 - 2nd International Symposium on Multidisciplinary Studies and Innovative Technologies, Proceedings*, Dec. 2018, doi: 10.1109/ISMSIT.2018.8567054.

[59] V. S. K. Devi and S. G. Srivani, "A DQ Synchronous Reference Frame Current Control for Grid Connected Photovoltaic Systems using Single Phase Cascaded H Bridge Multilevel Inverter," *International Journal of Engineering and Advanced Technology*, vol. 9, no. 2, pp. 2814–2822, Dec. 2019, doi: 10.35940/IJEAT.B3174.129219.

[60] T. Ahmadzadeh and I. Babaei, "Improved quasi-Z-source based three-phase three-level neutral point clamped inverter," *9th Annual International Power Electronics, Drive Systems, and Technologies Conference, PEDSTC 2018*, vol. 2018-January, pp. 99–103, Apr. 2018, doi: 10.1109/PEDSTC.2018.8343779.

[61] W. Liu, Y. Yang, E. Liivik, D. Vinnikov, and F. Blaabjerg, "Critical Parameter Analysis and Design of the Quasi-Z-Source Inverter," *2019 IEEE 2nd Ukraine Conference on Electrical and Computer Engineering (UKRCON)*, pp. 474–480, Jul. 2019, doi: 10.1109/UKRCON.2019.8879831.

[62] F. Guo, L. Fu, C. H. Lin, C. Li, W. Choi, and J. Wang, "Development of an 85-kW bidirectional quasi-Z-source inverter with DC-link feed-forward compensation for electric vehicle applications," *IEEE Trans Power Electron*, vol. 28, no. 12, pp. 5477–5488, 2013, doi: 10.1109/TPEL.2012.2237523.

[63] M. Muhammad, Z. Rasin, and A. Jidin, "Bidirectional Quasi-Z-Source inverter with hybrid energy storage for im drive system," *ISCAIE 2019 - 2019 IEEE Symposium on Computer Applications and Industrial Electronics*, pp. 75–80, Apr. 2019, doi: 10.1109/ISCAIE.2019.8743869.

[64] P. S. Praveena Krishna, S. Vishnu, A. Dash, V. B. Koreboina, and N. S. Jayalakshmi, "Investigation of bidirectional quasi Z-Source inverter for BLDC drive with modified shoot-through hysteresis current control in low power EV applications," *Cogent Eng*, vol. 10, no. 2, Dec. 2023, doi: 10.1080/23311916.2023.2283279.

[65] A. Abid, A. Bakeer, L. Zellouma, M. Bouzidi, A. Lashab, and B. Rabhi, "Low Computational Burden Predictive Direct Power Control of Quasi Z-Source Inverter for

Grid-Tied PV Applications," *Sustainability 2023, Vol. 15, Page 4153*, vol. 15, no. 5, p. 4153, Feb. 2023, doi: 10.3390/SU15054153.

[66] B. Seif Eddine, K. Djallel, and B. Seif, "New Strategy Control of Bidirectional Quazi Z Source Inverter with Batteries and Supercapacitors Energy Storage in Grid Connected Photovoltaic System," *International Journal of Power Electronics and Drive Systems (IJPEDS)*, vol. 8, no. 1, pp. 335–343, Mar. 2017, doi: 10.11591/IJPEDS.V8.I1.PP335-343.

[67] K. V. Priya and A. Aswini, "Simulation of Five Level Cascaded H-Bridge Multilevel Inverter with and without OTT Filter," *International Journal of Advanced Research in Electrical, Electronics and Instrumentation Engineering (An ISO*, vol. 3297, no. 2, 2007, doi: 10.15662/IJAREEIE.2016.0502003.

[68] K. D. Teryima, A. O. David, and S. T. Awuhe, "THD Analysis of an Overlapping Carrier Based SPWM For a 5- Level Cascaded H-bridge Multilevel Inverter," *International Journal of Advanced Science and Technology*, vol. 87, pp. 47–56, Feb. 2016, doi: 10.14257/IJAST.2016.87.06.

[69] O. Ozkara and A. Karaarslan, "Modified Three Phase Quasi Z Source Inverter using Sliding Mode Control Method," *ELECO 2019 - 11th International Conference on Electrical and Electronics Engineering*, pp. 1018–1024, Nov. 2019, doi: 10.23919/ELECO47770.2019.8990631.

[70] S. B. Sarode, S. G. Kadwane, R. K. Keshri, and A. Pathade, "Fuel Cell Based DC-AC Single Phase QZSI for Low Voltage Grid Utility," *2022 International Conference for Advancement in Technology, ICONAT 2022*, 2022, doi: 10.1109/ICONAT53423.2022.9725822.